NISTIR 6094

TESTING AND MODELLING OF FRESH CONCRETE RHEOLOGY

Chiara F. Ferraris
François de Larrard

Building and Fire Research Laboratory
Gaithersburg, Maryland 20899

United States Department of Commerce
Technology Administration
National Institute of Standards and Technology

ERRATA

1. **Figure 28 (p.46)**
   The vertical axis label should read $\mu \cdot 10^{-3}/\rho T$ instead than $\mu/\rho T$

2. **Equation 20 (p.46) should read**:

$$\mu = \rho T \bullet 1.08 \cdot 10^{-3}(S - 175) \qquad \text{for } 200 < S < 260 \text{ mm}$$

$$\mu = \rho T \bullet 25 \cdot 10^{-3} \qquad \text{for } S < 200 \text{ mm}$$

with ρ = density in kg/m^3 (in our case = 2400 kg/m^3)
T = slumping time in seconds
S = final slump in mm
μ = Viscosity in Pa·s

NISTIR 6094

TESTING AND MODELLING OF FRESH CONCRETE RHEOLOGY

Chiara F. Ferraris
François de Larrard*

February 1998

Building and Fire Research Laboratory
National Institute of Standards and Technology
Gaithersburg, MD 20899
* Guest researcher from Laboratoire des Ponts et Chaussées
Paris, France

DEPARTMENT OF COMMERCE
UNITED STATES OF AMERICA

National Institute of Standards and Technology
William M. Daley, *Secretary*
Technology Administration
Gary R. Bachula, *Acting Under Secretary for Technology*
National Institute of Standards and Technology
Ray Kammer, *Director*

EXECUTIVE SUMMARY

This report presents the results of an experimental program dealing with the rheology of fresh concrete. The three main goals were to:

- obtain rheological data on concretes of various mixture compositions;
- establish models to link mixture composition with rheological parameters, and
- develop a simple field test for determination of rheological parameters.

Approximately 80 mixtures (mortars and concretes, with and without High-Range-Water Reducer Admixtures (HRWRA)) were formulated and tested. The rheological characteristics of the mixtures were measured using a rheometer, developed at the Laboratoire Central des Ponts et Chaussées (Paris, France) named BTRHEOM, with parallel tests using the slump cone. The relationship between the torque and rotational speed of the rheometer is not linear, implying a non-linear relationship between stress and strain rate for concrete. An improved description of the rheological behavior of the material, better than the usual linear Bingham model, is provided by the Herschel-Bulkley model in the form $\tau = \tau'_0 + a\,\dot{\gamma}^b$, where τ is the shear stress, $\dot{\gamma}$ is the shear strain rate imposed on the sample, and τ'_0, a and b are characteristic parameters of the concrete being tested. Among other advantages, the non-linear model avoids the problem of a negative yield stress, which is sometimes encountered when the Bingham model is fitted to the test data. The "plastic viscosity" is defined from the characteristic parameters. However, for a certain number of applications, the Bingham approach may be retained as a first approximation.

Using the data obtained, the rheological characteristics of the mixtures were expressed as a function of their composition. A physical interpretation of the results is proposed. According to this interpretation, the yield stress term is a manifestation of friction between solid particles, while the "plastic viscosity" term results from viscous dissipation due to the movement of water in the sheared material. General forms for the models were deduced and the models were calibrated using the experimental data. The plastic viscosity appears to be controlled essentially by the ratio of the solid volume to the packing density of the granular mixture (including the aggregates and the cement). The yield stress is the result of an accumulation of contributions of each granular class, these contributions involving the size and roughness of the particles and their affinity for HRWRA. In addition to their predictive power, which must be confirmed with other experimental data, the models make it possible to understand several general tendencies observed in the rheology of cement-based materials when mixture proportions are varied, such as the influence of w/c ratio, cement content.

Finally, the development of a simple field test for estimating yield stress and plastic viscosity is described. The test in measuring the time necessary for the upper surface of the concrete in the slump cone to fall a distance of 100 mm. The details of the experimental setup and the procedure are described. The results of this test for all mixtures used in the program were analyzed. Semi-empirical models are proposed for estimating yield stress and plastic viscosity based on the results of this modified slump test. The area of application of the test for evaluation of the plastic viscosity is limited to concretes with a slump of 120 mm to 260 mm. If the validity of the modified slump test is confirmed in the future, it could be used for everyday quality control of concrete in the field.

TABLE OF CONTENTS

LIST OF TABLES

LIST OF FIGURES

NOTATION

τ	Shear stress
τ_0	Yield shear stress as defined by Bingham equation
τ'_0	Yield shear stress as defined by Herschel-Bulkley equation
μ	Plastic viscosity as defined by Bingham equation
μ'	Plastic viscosity as calculated from the Herschel-Bulkley parameters
$\dot{\gamma}$	Shear strain rate
a, b	Parameters of the Herschel-Bulkley equation (theoretical)
Γ	Torque measured in the rheometer
Γ_0	Torque corresponding to a zero-value of the angular velocity
N	Angular velocity
A, B	Parameters that depend on the rheometer geometry and the concrete (Herschel-Bulkley equation)
R_2, R_1	Radii of the rheometer
Φ, Φ_1, Φ_i	Solid volume fraction of a constituent
Φ^*, Φ_1^*, Φ_i^*	Packing density of a dry mixture (maximum value of Φ for close packing)
f, g	Undefined functions
γ	Virtual packing density
y_i	Proportion by volume of size i, i.e., ratio of volume of size class i to the total solid volume
n_i	number of size class i
a_{ij}, b_{ij}	Interaction functions describing binary relaxation and wall effect, respectively
β_i	Virtual packing density of size class i compacted alone
d_i, d_j	Diameter of granular size classes i and j
K	Compaction index
K_i	Compaction index for each size class i
K_i	Compaction index for each size class i for de-aired concrete
K_s, K_a, K_c, K_{sf}	Compaction indices for fine and coarse aggregates, cement and silica fume respectively
c	Maximum volume concentration of cement in a paste
$SP\%$	Dosage of HRWRA (percent by mass of cement)
ρ	Density
g	Acceleration of gravity
h	Height of slump cone
s	Slump measurement using the slump cone
T	Slump time

1. INTRODUCTION

1.1. Scope of research

This report presents the results of an experimental program dealing with the rheology of fresh concrete. The three main goals were to:

- obtain rheological data on concretes produced with various mixture compositions;
- establish models to link mixture composition with rheological parameters, and
- develop a simple field test that will determine rheological parameters.

Chapter 2 presents the characteristics of the material components that were used, the experimental plan that was followed, and the analysis of the results. A new relationship is given in Chapter 3 between shear stress and shear strain rate, and the flow of the fresh concrete. Chapter 4 presents an analysis of the relationships between rheological characteristics and concrete composition, and describes models developed for the plastic viscosity and the yield stress. Finally, Chapter 5 deals with a modification of the standard slump cone test aimed at providing an experimental evaluation of the Bingham parameters by applying a simple test that is affordable and easy to use as part of quality control testing. This test is not intended to replace a true rheometer, but rather to expand and facilitate the collection of rheological data, particularly in the case of high-performance concretes for which the classic slump test is inadequate.

1.2. Recent developments

In the following section a brief review of recent developments in the characterization of the rheological properties of concrete is presented. Studies on the rheology of fresh concrete, from a materials science approach, are just beginning to appear. In fact, the concretes that are easier to describe by such an approach, i.e., concretes that are sufficiently fluid, have only been commercially used recently. Previously, it was considered adequate to use an engineering approach for characterizing rheological properties, consisting of subjecting a concrete sample to a more-or-less controlled loading and deriving an index (slump, flow time, compacting factor, etc.) to classify the mixtures in terms of workability. This approach is limited as the classifications obtained by using different tests vary substantially [42].

Tattersall was one of the pioneers of concrete rheology when, in 1991, he proposed using an instrumented mixer to obtain a more complete characterization of the flow characteristics of fresh concrete [1]. He proposed describing the behavior of fresh concrete using the Bingham model in the following form:

$$\tau = \tau_0 + \mu \dot{\gamma} \qquad (1)$$

where τ is the shear stress applied to the material (in Pa), $\dot{\gamma}$ is the shear strain rate (also called the strain gradient) (in s^{-1}), τ_0 is the yield stress (in Pa) and μ is the plastic viscosity (in

Pa·s). The last two quantities (the Bingham parameters, τ_0 and μ) characterize the flow properties of the material. However, in Tattersall's apparatus, the velocity field is unknown and complex due to the lack of symmetry. Therefore, he limited himself to an empirical description of the material's behavior, by using the relationship between the torque and the rotation speed of the mixing blades.

The same approach was pursued by Wallevik, who attempted to improve on Tattersall's apparatus by returning to the more classic geometry of a viscometer with coaxial cylinders (BML viscometer [2]). Unfortunately, this instrument's design did not consider the reasons that led to the shape of the blades in Tattersall's apparatus. Tattersall's blades were designed to overcome the natural tendency of concrete to segregate by creating a vertical movement through the tilt of the blades. The movement of the concrete in the BML viscometer is essentially horizontal, and places more than half of the total volume of concrete in "dead" zones, in which the concrete is not sheared during the test. Thus, segregation can occur through the migration of fine particles from the dead zones to the sheared zones, resulting in an underestimation of the rheological characteristics.

After the characteristics and shortcomings of these devices were analyzed [3], the BTRHEOM rheometer was developed [3, 4, 8]. Designed on the basis of both scientific and practical requirements, this rheometer has the ability to provide fundamental rheological values, while being portable and usable on the job site.

Hu validated the measurements obtained with the BTRHEOM rheometer — as far as it is possible to do so — by performing finite element calculations and comparative tests with all existing rheometers [7]. It appears that the Bingham parameters are determined with an uncertainty that does not exceed 10%, which is satisfactory for a test of this kind. Once the basic characteristics of the apparatus were established, it remained to put it to use to increase the database of available knowledge on concrete rheology.

1.3. Potential benefits of this study

It was shown that the BTRHEOM rheometer is a valuable tool for monitoring concrete rheological properties [5]. The rheometer makes it possible to show the loss in workability over time for a single sample, and to provide a diagnosis of the *causes* of these changes, whether linked to absorption of water by the aggregates or to incompatibility between the cement and the HRWRA [6]. However, for the rheological approach to become an integral part of concrete engineering, two information gaps have to be bridged (see Figure 1).

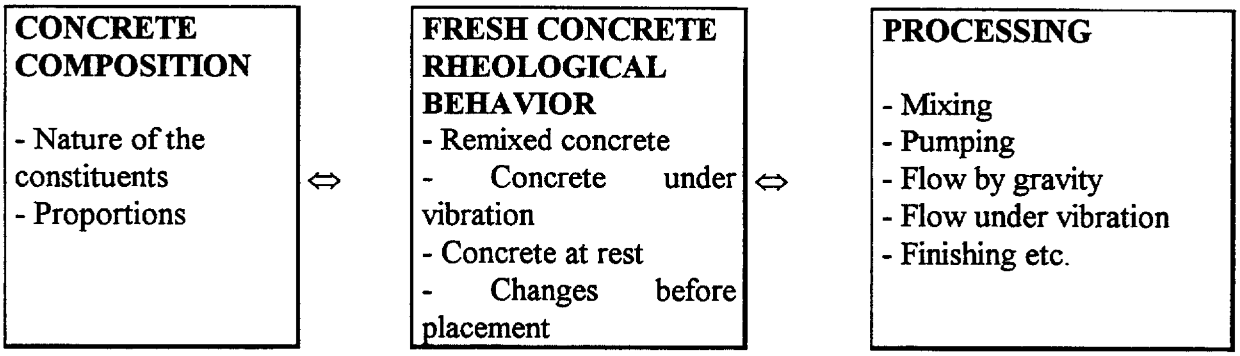

Figure 1. Gaps, i.e., missing links, in the knowledge of concrete rheology to be filled to make rheology truly usable by the engineer

First, it is necessary to understand how the processing parameters are linked to the rheological behavior of the concrete. For example, it seems that concrete pumpability is controlled by plastic viscosity [7,8]. Also, it would be interesting to determine if the stability of fresh concrete placed at an angle (or on a slope) is controlled by the yield stress [7]. One could establish requirements for concrete rheological characteristics that would make it possible to empty a concrete bucket within a given time based on finite element calculations of the same type as those used by Tanigawa et al. [9,10].

Second, efforts must be made to *link the rheology of the concrete to its composition.* This is one of the objectives of the present study. When this objective is reached, the engineer will be able, at the mixture design stage, to optimize the mixture proportions taking into account placing methods and structure types.

2. EXPERIMENTS

2.1. Materials

2.1.1. Aggregate

The principal aggregate used in this study is from silica-limestone alluvial deposits from the area of Washington, D.C., USA. It is rather rounded in shape. The two sizes (0-4 mm sand and 4-10 mm coarse aggregate) have a specific gravity (in the dry state) of 2.61 measured following ASTM C127 [11] and C 128 [12]. The respective water absorptions are 0.6 and 0.7% (measured using ASTM C-127 [11] and C128 [12]), the dry packing density values are 0.715 and 0.612 (measured using a vibrational procedure[1] [13]). To assure continuity in the size distribution of the mixtures, a round fine sand (0.106 mm to 0.075 mm) from Ottawa, Illinois, USA[2] (density 2.65, water absorption 0%, packing density 0.659) was used. This sand corrected the deficiencies in gradation of the alluvial sand by adding fine particles with diameters between the fine sand fraction and the largest cement particle sizes. The grading curves of the aggregates, obtained by sieving, are given in Figure 2. For the mortars, the aggregates were screened to give a maximum 2.5 mm diameter (Figure 2).

In order to model more precisely the contribution of the sand to the packing density of the mixtures, the packing densities of three granular fractions of the sand were also measured. The values were 0.625 for the coarse fraction (1.25 mm to 4 mm), 0.621 for the middle fraction (0.315 mm to 1.25 mm) and 0.581 for the finest fraction (0.125 mm to 0.315 mm).

The packing density mentioned in the paragraph above is defined as the maximum solid material in a unit volume. This factor is 1 for solid material (no air) and 0 for air only.

---

[1] 791 g of material placed in a metal cylinder 76 mm in diameter surmounted by a piston applying a vertical pressure of 10 kPa, subjected to vibration for one minute at maximum amplitude with a SYNTROM-FMC-VP 51[2] vibrating table.

[2] Brand names, names of manufacturers and equipement are identified in this report to adequately describe the experimental procedure. Such an identification does nor imply recommendation or endorsement by the National Institute of Standards and Technology, nor does it imply that the material identified is necessarily the best available for the purpose.

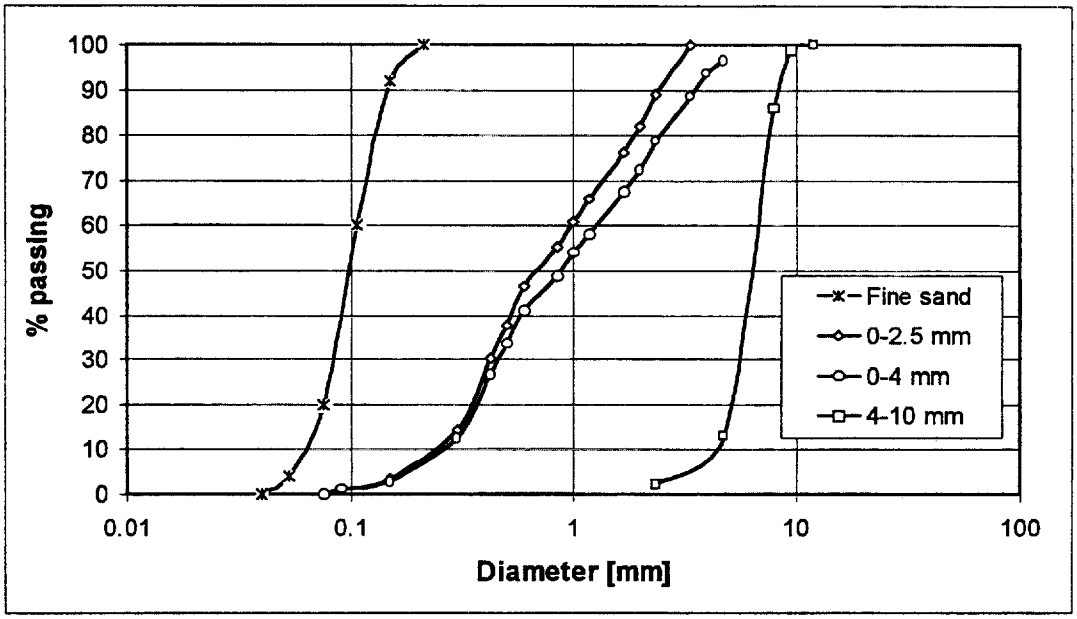

Figure 2. Size distribution of the aggregates used in the mortars and concretes

2.1.2. Cement

A Type I/II portland cement (ASTM C150 [14]) from Lehigh Portland Cement Co. (Allentown, PA)[2] was used for all of the tests. Its specific gravity was measured to be 3.15. Its compressive strength was 62 MPa at 28 days (following the ISO mortar test [15]). The chemical composition is given in Table 1 and the size distribution (measured in alcohol using a laser granulometer) is given in Figure 3. The packing density, calculated from the water demand test described in [13], is 0.565 without admixture and 0.606 in the presence of 1% HRWRA (total solid by mass of cement).

2.1.3. Silica fume

Silica fume, obtained from Elkem[3], was used in slurry containing 54% solids by mass. The specific gravity of the solid was assumed to be 2.2. The size distribution measured using the sedigraph method in the presence of lime water and 4% HRWRA shows the expected high degree of fineness of the silica fume (which was 77% by mass finer than 0.25 μm, Figure 3). The chemical composition of the silica fume is given in Table 1.

---

[3] same comment than for footnote 2 on page 4

Table 1: Chemical composition of the cement and the silica fume in percentage by mass, as determined at LCPC

REFERENCE		**Cement**	**Silica Fume**
Silica	SiO_2	21.29	96.68
Aluminum Oxide	Al_2O_3	4.42	0.45
Titanium Oxide	TiO_2	0.22	--
Ferric Oxide	Fe_2O_3	2.87	0.22
Calcium Oxide	CaO	63.83	1.24
Magnesium Oxide	MgO	1.78	0.24
Sodium Oxide	Na_2O	0.21	0.24
Potassium Oxide	K_2O	0.76	0.49
Sulfuric trioxide	SO_3	3.03	--
Chlorine	Cl	--	--
Sulfur	S	0.07	--
Insoluble Residue	RI	0.20	--
Loss on Ignition at 1000°C	PAF	0.77	--
Manganese oxide	MnO	0.05	0.04
Total		**99.50**	**99.60**

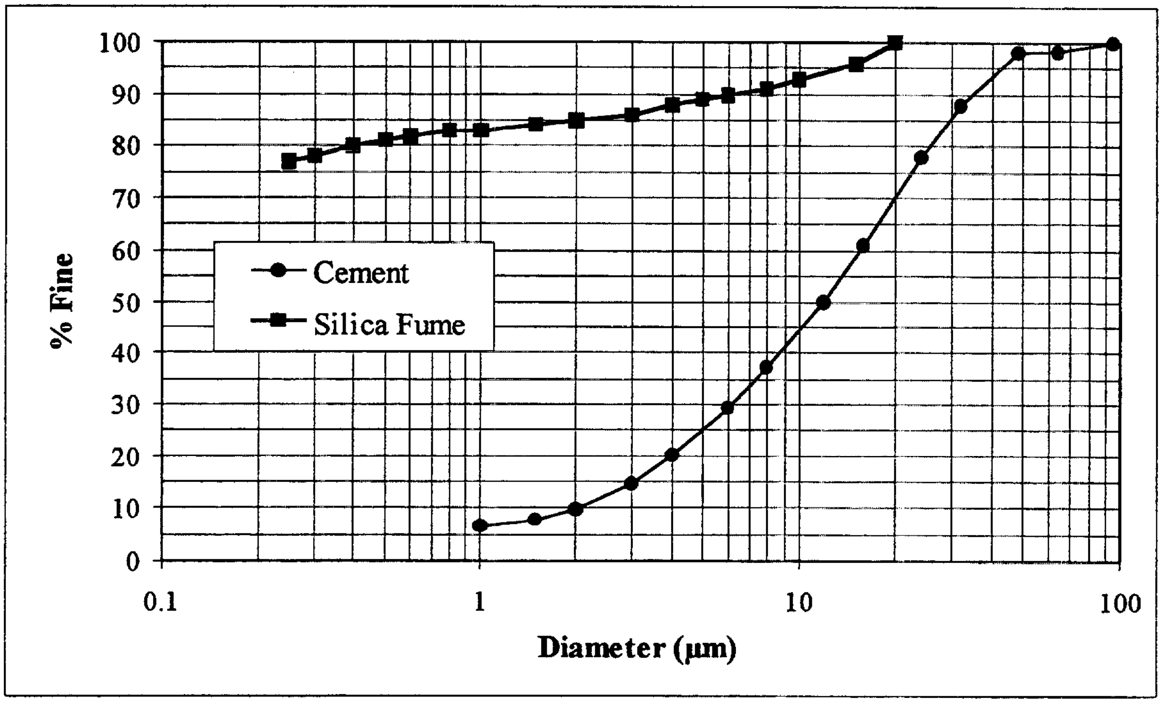

Figure 3. Size distribution of the binders used in the mortars and concretes

2.1.4. HRWRA

A sulfonated naphthalene in an aqueous solution with 40% dry extract by mass (commercial name[2] is DARACEM 19 made by the W. R. Grace & Co.) was used as a HRWRA in half of the mixtures. For the rest of the mixtures no HRWRA was used.

2.2. Methodology

2.2.1. Preparation of the concretes

The concretes were made using a vertical-axis pan mixer (manufactured by Lancaster International, model LWD[4]) with a maximum capacity of 16 liters. The aggregates were oven dried before use. All of the dry materials were introduced into the pan-mixer and mixed dry for one minute, then the following mixing schedule was used:

Ordinary Concretes:
- With the mixer running, the water was added at an approximately constant rate during a period of 30 seconds;
- Mixing was continued for another two minutes, and the mixture was discharged from the pan.

Concretes with HRWRA:
- The water, to which one-third of the total dose of HRWRA had been previously added, was added, at an approximately constant rate, during a period of 30 seconds, while the mixer was running;
- Mixing was continued for another two minutes;
- The remaining portion of HRWRA was slowly added to the mixture over a period of 30 seconds, with the mixer running;
- Dispersion of the HRWRA was achieved by an additional one minute of mixing, and the mixture was discharged from the pan

The total mixing time was 3.5 minutes for the concretes without HRWRA, and 5 minutes for the concretes with HRWRA.

For the concretes with silica fume, the silica fume slurry was added to the dry materials before mixing was started, except for the mixture with the highest amount of silica fume (FS 30), for which the slurry was previously mixed with water containing the first dose of HRWRA.

The density of the fresh concrete was measured by weighing a 2 liter-cylinder. The cylinder was filled, and the concrete was consolidated in accordance with ASTM C 138-92 [16]. This test does not provide a direct measurement of the air content, but it gives an estimate of the

---

[4] Same comment as on footnote 2 on page 4

density of the fresh concrete that is needed for other calculations. The slump was measured following ASTM C 143-90 [17], except that the apparatus was modified as described in Chapter 5 to provide information on the rate of slump. The effect of these modifications on the final slump was found to be negligible.

2.2.2. Using the BTRHEOM rheometer

The experimental plan was designed so as to make a reasonable survey of the full range of workable mixtures of the chosen components. It was expected that segregation problems would be encountered for some compositions. For this reason, the following measurement procedure was selected. After the rheometer chamber was filled, the material was vibrated for 15 seconds at a frequency of 40 Hz. Then, rotation of the blades was begun and increased to a maximum velocity of 0.8 rps (revolution per second). The rotation velocity was reduced in four stages distributed nearly uniformly over the interval from 0.8 to 0.2 rps. Five torque measurements were made at each velocity, and the rheological characteristics of the concrete without vibration were determined. The whole test lasted about 3 to 4 minutes. Because of the abnormal characteristics of a certain number of mixes, it was decided not to perform rheometer tests under vibration since interpretation of the results would have been impossible. At the end of each rheometer test, the appearance of the top horizontal surface of the concrete was noted. This was done by assigning a grade from 0 to 3 based on a qualitative assessment of the amount of bleeding and the segregation caused by rise of the gravel (0 = no bleeding, 3= severe bleeding)

The BTRHEOM is sealed by a fabric ring seal. This seal creates friction that increases the measured torques. Therefore, before each test of a given mixture, calibration was performed using water to measure the contribution of the seal to the overall torque measurement. The concrete test was then corrected automatically by the software (ADRHEO) provided with the rheometer using the protocol set forth in Ref. [5].

2.3. Experimental studies

The experimental plan consisted of systematically characterizing a reasonable range of the mixtures that could be made from the three basic materials: coarse aggregates, combined sand (a mixture of alluvial sand and fine silica sand in fixed proportions) and cement. Based on a certain number of dry compositions (considering only the volumetric fractions of solid materials), three wet mixtures were made by varying the water content so as to cover the range of consistencies that could be characterized by the rheometer. The lower limit was found to corresponded to a slump of about 100 mm for mixtures without HRWRA [3], while the upper limit was reached when bleeding was considered to be excessive. Few mixes were also done using silica-fume as described in section 2.3.4.

2.3.1. Ordinary concretes

In this series, both the coarse aggregates and the two sands were used, with the exception of the HRWRA. The optimum mixture (called *central*, hereafter) was calculated using software (René-LCPC version 5) developed at Laboratoire des Ponts et Chaussées (LCPC) [13]. The composition of the central mixture was designed to obtain the maximum dry packing density, but with a slight excess of cement in order to minimize the bleeding in all of the mixtures under-dosed with sand. It was the optimization of the packing density at a fixed cement content that led to adopting the proportion of fine sand to alluvial sand of 30% by mass, a value that was maintained throughout the series. The other dry mixtures were generated on the basis of the *central* mixture by changing one or both of the following two parameters: the volumetric proportion of cement and the volumetric ratio of sand to total aggregate[5] (see Figure 4). It should be noted that the latter ratio was 100% for three dry combinations that were mortars. For these mixtures, to avoid the bleeding that was produced with a cement dosage equivalent to those for the concretes, the proportion of cement by volume was shifted increased as shown in Figure 4. Finally, the combination corresponding to the lowest dosage of cement and the highest dosage of gravel was not made because of the segregation problems, i.e., sedimentation and bleeding, that would have unavoidably occurred.

In order to determine the dosages of water to produce the desired slumps, we began by adopting a dosage corresponding to the porosity of the dry system (provided by the René-LCPC software) plus a fixed additional amount of water. Based on the slump obtained, the water dosage was then reduced or increased, the objective being to obtain three concretes (or mortars) of different consistencies for each dry combination. This procedure has the advantage of conserving materials. On the other hand, we sometimes reached the operating limits of the rheometer. However, knowledge of the limits of applicability of the methodology was also an objective of this study. The composition of mortar and concrete mixtures obtained are given in Appendix I. In addition to the dry compositions (given in mass percentages), the proportions by mass per cubic meter, based on the assumption that the entrapped air content was 1%, are also presented. It should be noted that two additional concretes were produced for the *central* mixture, bringing to a total of five the number of concretes having the optimum dry composition but variable water content. In Appendix I, the numbers in the mixture identification names correspond to the numbers shown in Figure 4.

---

[5] Or the ratio of sand to (sand + gravel).

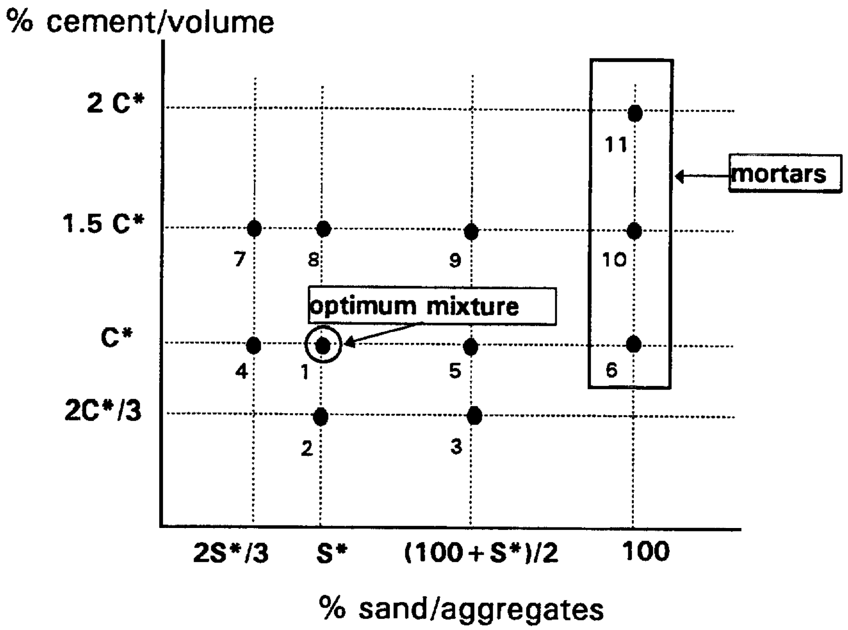

Figure 4. Experimental plan. Method of calculating the proportions of dry materials in the series of ordinary concretes and concretes with HRWRAs. The cement content of the mortars (compositions 6-10-11) have been increased to reduce bleeding. S* is the volumetric ratio of sand to total aggregate and C* is the volumetric proportion of cement of the optimum or *central* mixture.

2.3.2. Concretes with admixtures

In this category of concretes, dry mixtures were generated on the basis of the same mixture design principle as used for mixtures without HRWRA. However, an attempt was made to obtain a higher range of slumps, as is the case in industrial practice with concretes containing HRWRA. To all of these mixtures, 1% of dry extract of HRWRA based on mass of cement was added. This amount chosen on the basis of results from a series of "mini-slump" [18] type tests on cement paste (Figure 5), is probably close to the saturation dosage based on the AFREM grout method [19], developed at LCPC. The saturation dosage could be interpreted as the maximum dosage of HRWRA beyond which no further increase in the mini-slump value is observed. This dosage of HRWRA ensured against the rapid loss of workability, which would have jeopardized the tests, as well as assuring maximum deflocculation of the cement particles in all of the mixtures, regardless of their composition. However, this high dosage of HRWRA frequently results in excessive bleeding. Moreover, for the lean compositions (low cement content), such as those of groups BHP2 and BHP3, it was not possible to obtain a high slump. Apparently the water that was in excess of the porosity of the dry mixture, bled instead of separating the particles and "lubricating" the mixture. The compositions of the mortars and concretes of the series with HRWRA are shown in Appendix II.

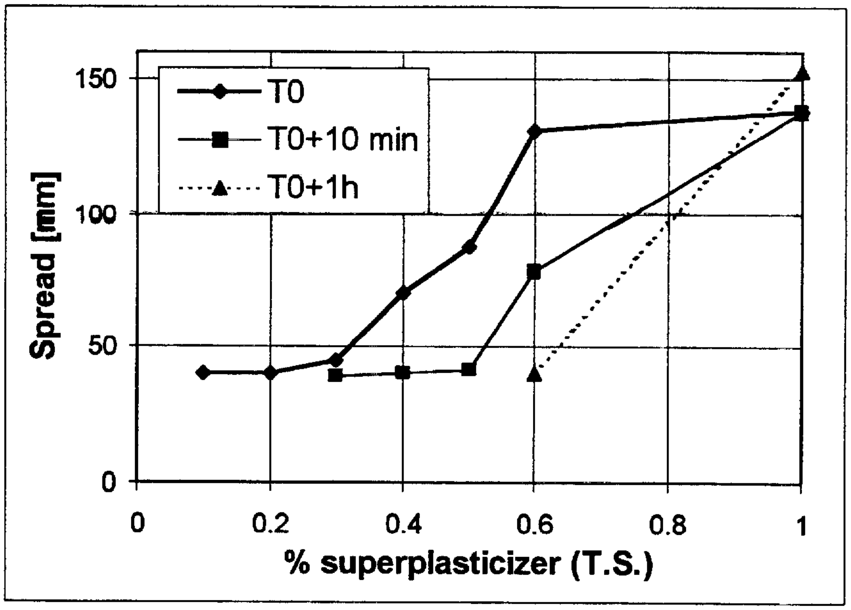

Figure 5. Mini-slump tests on cement pastes in the presence of HRWRA. A spread of 40 mm corresponds to zero slump because it corresponds to the diameter of the base of the mini-cone used. TS = total solid content of the HRWRA (% by mass). T0 is the initial time, just after mixing, at which the mini-slump was measured. The other two curves indicate the mini-slump value after 10 minutes (T0+10 min) and after 1 hour (T0 +1h).

2.3.3. Intermediate concretes

Although the experimental program was mainly devoted either to concretes without HRWRA or with high dosages of HRWRA, it was also important to examine the effects of intermediate HRWRA dosages, at least, for a limited number of mixtures. Most modern commercial concretes are found in this range. Therefore, four mixtures were generated by simple linear interpolation between the *central* mixture without HRWRA and its corresponding mixture with HRWRA. Thus, the concrete called "80% BO" corresponds to a mixture (by mass) composed of 80% of the central mixture without HRWRA and 20% of the central mixture with HRWRA (Appendix III).

2.3.4. Silica fume concretes

The silica-fume concretes are another example of mixtures that are of practical interest but are difficult for the rheologist to deal with, because the silica fume particles are for the most part finer than one micrometer (Figure 3), and so are colloidal. At this scale, surface forces can play an important role, making their behavior more complex. Therefore, from the central mixture with HRWRA, we generated four additional concrete mixtures with dosages varying from 7.5% silica fume by mass of the cement to a maximum of 30%, by incremental steps of 7.5%. Obviously, the highest dosage is clearly excessive (too expensive and excessive changes in other properties) for most practical uses of high-performance concrete. The purpose was simply to scan a large range of silica fume dosages and to obtain mixtures in which the silica fume would contribute significantly to the rheology of the system. The dosage of HRWRA was increased at the rate of 4% of the mass of silica fume to maintain a mixture saturated with HRWRA. The compositions of the silica-fume concretes are shown in Appendix III. The quantities of silica fume given in Appendix III are those of the slurry, which is 54% solids by mass.

3. RESULTS AND ANALYSIS OF THE RHEOLOGICAL DATA

3.1. Results

The test results are given in Appendix IV for ordinary concretes, Appendix V for concretes with admixtures, and Appendix VI for concretes with silica fume and with intermediate dosages of HRWRAs. For each mixture, the data collected from the measurements of the modified slump tests, the density, and the Bingham parameters are given. Also the parameters calculated using the Herschel-Bulkley function are listed (see section 3.1.4). Visual observations reported bleeding and segregation, the qualitative ranking (0 to 3) is included in the tables (0= good and 3 = worst case).

3.1.1. Slump test results

Slumps were obtained throughout the entire range from 0 mm to 290 mm (for self-leveling mortar). For the most fluid mixtures, the slump flow was also measured (i.e., the average diameter of the spread after stabilization, measured parallel to the sides of the rectangular metal plate on which the tests were performed). Some concretes exhibited segregation, manifested by the accumulation of coarse aggregates surrounded by a "lake" of mortar. Within each group corresponding to the same dry mixture, the slump increased with the dosage of water, except for the BHP1 and BHP4 groups. Overall, it was found that the sensitivity of the slump test to the amount of water varied from one series to the other.

3.1.2. Rheometer results

The rheometer test was performed on all of the mixtures that were made. However, for some mixtures, because the slumps were too low or the size distributions were too far from the *central* mixture, it was not possible to obtain usable measurements, i.e., the shearing was not uniform. The mixtures with bold lettering in the tables of Appendix IV and Appendix V are those for which the rheometer measurements were valid. Some concretes, such as those of the BHP8 series, which had HRWRAs and high cement contents, exhibited the peculiarity of being self-leveling (very low yield stress), along with high plastic viscosity, which was visually apparent by their extreme slowness in reaching their equilibrium position during the slump test. The torque necessary to shear them at the maximum velocity (0.8 rps) sometimes exceeded the capabilities of the rheometer. Hence, after a nonproductive test, the test was repeated while limiting the range of the shear rate, called "reduced shear rate" tests (Appendix V). Only one test was conducted for each mixture, therefore no calculation of uncertainty can be made. From previous tests [7], the error on the torque and the rotation speed can be estimated to be less than 1%.

The intensity of bleeding varied a great deal from mixture to mixture. In the series of concretes without HRWRA, all the concretes with low cement contents (groups BO2 and BO3 (Appendix IV) exhibited appreciable bleeding during the course of the rheometer test. A majority of the concretes with HRWRA also displayed the same phenomenon, particularly when the slump was increased by adding water. The "intermediate" concretes behaved similarly, while the silica fume concretes remained homogeneous during the tests, confirming the well-known stabilizing character of ultra-fine particles.

The negative effect of the HRWRA on the cohesiveness of the concretes was also observed as the segregation increased when the amount of gravel was increased. This consequence of the dilatant property of the mixtures [7] was, as might have been expected, manifested particularly for the mixtures that had HRWRA and high coarse aggregate content.

3.1.3. Analysis of the results using the Bingham model

For each rheometer test, a linear regression analysis was performed on the values of the net torque (i.e., the torque after subtracting the contribution of the seal) as a function of the rotation velocity in order to deduce the Bingham parameters, the yield stress and plastic viscosity, in accordance with the procedure given in ref. [7]. The results are given in the tables in Appendix IV to VI.

The plastic viscosity values were distributed over a wide range. Generally, the mixtures with HRWRA have higher plastic viscosities than those without HRWRA. This is attributed to the HRWRAs having a greater effect on the shear yield stress than on the plastic viscosity, while water reduction causes a notable increase in both parameters [1,7]. In the series of intermediate concretes, while the slumps remain in the same range, it is striking to observe how the plastic viscosity increases as the *central* mixture with HRWRA is approached (see Appendix VI). On the contrary, incorporation of silica fume makes it possible to negate the effect that lowering the water dosage has on plastic viscosity, in accordance with the known filler effect. When the *central* mixture with HRWRA (BHP1C) is compared with the mixture richest in silica fume (FS30), reducing the water/binder ratio from 0.38 to 0.24, decreases the plastic viscosity from 530 to 400 Pa·s. This study confirms the beneficial effect of silica fume on the plastic viscosity of high-performance concretes [20] because a lower plastic viscosity makes the placement easier.

Among concretes having slumps equal to at least 100 mm, the yield stresses that are obtained remain lower than 2000 Pa (Appendix IV-VI), which was expected on the basis of past experience [7]. On the other hand, *negative yield stresses are obtained with seven mixes*, sometimes with values below - 300 Pa, which are not explainable by the uncertainty associated with measurement (on the order of 100 Pa). A negative yield stress also implies that the data have a high degree of non-linearity and Bingham model cannot, therefore, be used to extrapolate the yield stress. Moreover, examination of the curves of the torque as a function

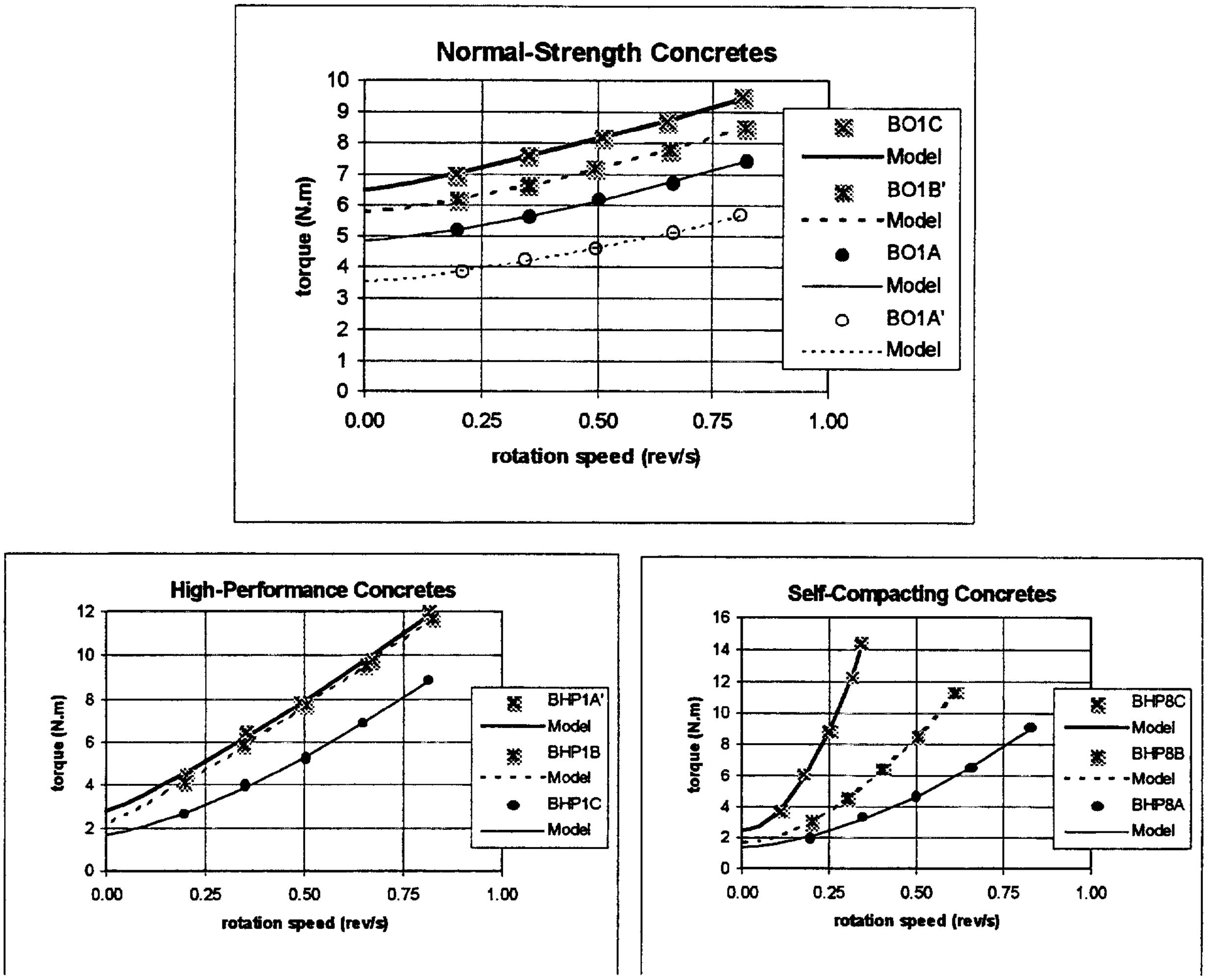

Figure 6. Measurement of torque as a function of the angular velocity for three groups of concrete, and fit with a model of the Herschel-Bulkley type. In each group, the curves are ranked as expected as a function of the water content of the mixtures (i.e., the torque decreases as the water content increases).

of the angular velocity of the rheometer blades shows a varying degree of nonlinearity (see Figure 6).

3.1.4. Fresh concrete as a Herschel-Bulkley material

Based on the above analysis using the Bingham model, it was necessary to develop a non-linear model to represent the flow behavior. Prompted by an approach borrowed to describe the "rheology of mud" [21], a granular material that has a number of similarities to concrete, we applied the Herschel-Bulkley model. This provides a relationship of shear stress to shear strain rate based on a power law [22]:

$$\tau = \tau'_0 + a\,\dot{\gamma}^b \qquad (2)$$

where τ is the shear stress, $\dot{\gamma}$ is the shear strain rate imposed on the sample, and τ'_0, a and b are the new characteristic parameters describing the rheological behavior of the concrete. The relationship between the torque and the angular velocity of the rheometer is similar to the previous equation, and is calculated by integration of the function relating the velocity field and the torsional motion imposed by the geometry of the test. It is in the following form:

$$\Gamma = \Gamma_0 + A\,N^b \qquad (3)$$

where Γ is the torque, Γ_0 is the minimum torque necessary to shear the sample, N is the angular velocity in revolutions per second and A and b are the parameters that depend on the concrete and the dimensions of the apparatus. By following the same calculation steps as in the analysis of the test using the Bingham model [7], one obtains the following formulas for the characteristic parameters relating to the concrete:

$$\begin{aligned} \tau'_0 &= \frac{3}{2\pi(R_2^3 - R_1^3)}\Gamma_0 \\ a &= 0.9\frac{(b+3)}{(2\pi)^{b+1}}\frac{h^b}{\left(R_2^{b+3} - R_1^{b+3}\right)}A \end{aligned} \qquad (4)$$

where R_1 and R_2 are the interior and exterior radii of the concrete sample in the rheometer (equal to 20 mm and 120 mm, respectively), and h is the height of that sample (equal to 100 mm). The coefficient 0.9 in the equation for the coefficient a takes into consideration the resistance effect of the friction of the side walls on the flow of the concrete in the apparatus.

This Herschel-Bulkley model was fitted to the experimental curves of torque versus angular velocity. The Herschel-Bulkley model fits the experimental curves quite well. Examples of these curves are given in Figure 6, and the values of the rheological parameters for the various mixtures appear in the tables in Appendix IV to VI. One finds that all of the new yield stress (τ'_0) values calculated using equation (4) are positive. As to the values of the parameter b, they are generally greater than one (1.53 on the average for the concretes without HRWRA and 1.36 for the concretes with HRWRA), which clearly shows that the actual behavior of the fresh concrete generally differs from the linear behavior described by the Bingham model.

3.1.5. Relationship between slump measurements and the Herschel-Bulkley yield stress

The connection between the Herschel-Bulkley yield stress and the slump has been shown both theoretically and experimentally [7, 23]. The present tests confirm this relationship (Figure 7). If all the results obtained, including the concrete without HRWRA for which the slump was less than 100 mm are used, Figure 7 shows that the data can be approximated by a single curve. This suggests that the range of validity of the rheometer tests, in regard to the "new" yield stress (Herschel-Bulkley), extends beyond concretes having a very plastic consistency, i.e., high slump or low yield stress. We were also interested in the final slump flow, which has been considered to provide a better measurement (than the standard slump) of the consistency of self-leveling concretes [24]. Self-leveling concretes have a slump value of 260 mm or higher. Excluding the mixtures whose slump tests exhibited segregation by accumulation of coarse aggregates in the middle of the concrete, it is found that the slump flow is related to the yield stress (see Figure 8). Therefore, the measurements obtained with the slump test support use of the Herschel-Bulkley model for analysis of rheological tests.

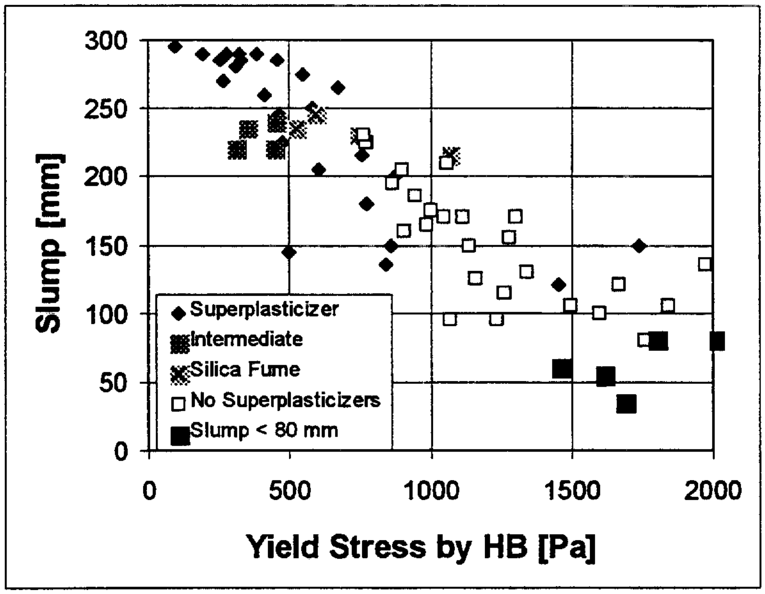

Figure 7. Relationship between yield stress from the Herschel-Bulkley (HB) model and slump for all of the mixtures tested.

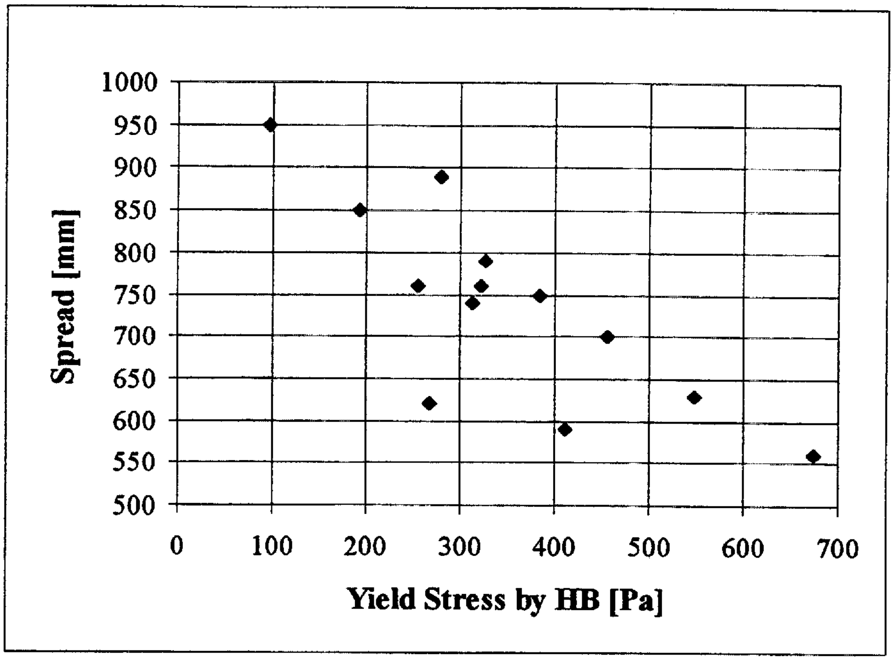

Figure 8. Relationship between yield stress from the Herschel-Bulkley (HB) model and slump flow (spread) for the self-leveling concretes.

3.2. Discussion

3.2.1. Non-linear behavior

In order to minimize segregation during rheometer testing, we adopted (see section 2.2.2) a procedure that consisted of measuring five points in the selected range of angular velocity. The drawback of this choice appeared afterwards when we realized that it would be necessary to determine by regression three parameters, instead of two, based on these five experimental points. Because three parameters must now be determined using only five points, the number of degrees of freedom is very low. Therefore, the uncertainty in fitted parameters is greater and it is more difficult to conclude with certainty that the parameter *b* differs from 1.0. In order to judge the accuracy obtained on the fitted parameters, we used one of the concrete mixtures tested in accordance with the procedure previously defined (test B08C) and repeated the test using an identical procedure, except that the range of the angular velocity was extended in both directions (i.e. one point was added at a higher velocity and one at a slower velocity). The measurements were still done by decreasing velocity. The result of this additional test (BO8Cbis) is shown in Figure 9.

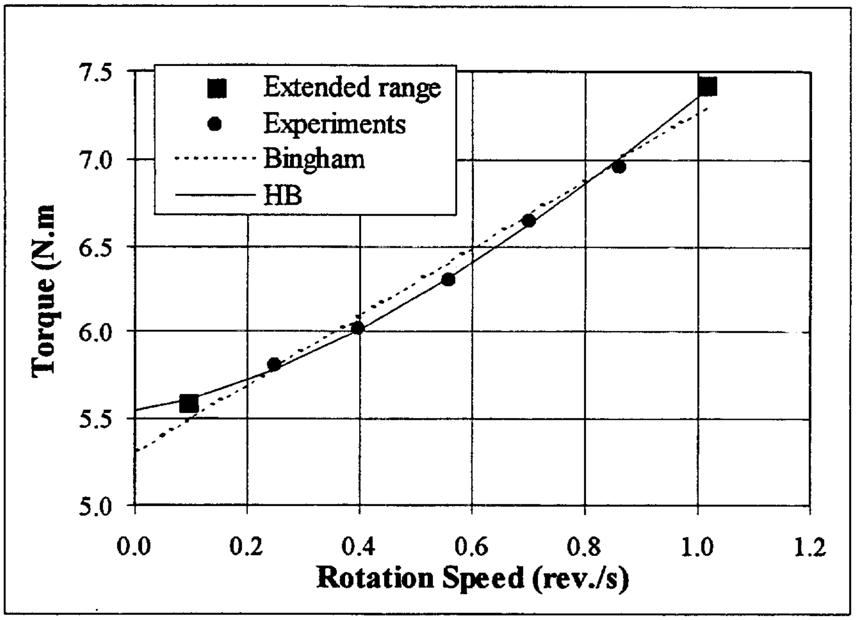

Figure 9. Measurements of torque as a function of rotational speed, for the BO8C mixture. The test was repeated using a larger range of rotational speed.

A considerable difference is found between the torque values obtained in the two tests (regular procedure, BO8C, and the extended range, BO8Cbis, of shear strain rates), which is shown by the marked differences in the yield stress in Table 2. Shearing the concrete at higher velocities has a tendency to promote segregation [5]. Therefore, this further justifies the precautions taken in the procedure that was adopted. On the other hand, when the results of the second test, BO8Cbis, are considered in isolation, it turns out that the Herschel-Bulkley parameters are not very sensitive to the number of points considered, whether it consists of a total of seven points or is reduced to the five central points, as in the standard test. Thus, if all of the tests had been performed in the same range of shear strain rate, but with a greater number of measurement points, the rheological parameters obtained would probably not have been very different from those found.

Table 2. Calculation of Herschel-Bulkley parameters from the BO8Cbis test using only 5 points (limited range of shear) and using 7 points (extended range) and the value measured on BO8C (limited range of shear).

		Shear range (1/s)	rate τ'_0 (Pa)	a (Pa·s^b)	b
BO8C	5 pts	0.31-6.5	1841	42.0	1.66
BO8Cbis	5 pts	0.31-6.5	1539	36.1	1.43
BO8Cbis	7 pts	0.12-7.6	1535	34.7	1.47

Another question concerns whether the centrifugal force during the tests could explain the nonlinear behavior. The contribution of the outer layers to the resistant torque of the sample (from which the distance to the axis is greater than half of the radius of the apparatus) is predominant, and the outer layers could have an over-concentration of aggregate. We believe that the non-linearity is not due to the effect of the centrifugal force for the following reasons:

- The acceleration due to the centrifugal force is at most 3.0 m/s^2 (for an angular velocity of 0.8 rps and a radius of 0.12 m), i.e., less than a third of the acceleration due to gravity. Thus, any radial segregation due to the circular movement should be less than that which inevitably results from gravity.

- Mixture BHP8C exhibits a strongly nonlinear behavior ($b = 1.88$). However, the maximum rotation velocity during the rheometer test was only 0.34 rps (corresponding to a maximum acceleration of 0.5 m/s^2). In addition, given the extreme plastic viscosity of this material, it is hard to see how the gravel could have segregated during the test.

- Finally, a comparison of the behavior of mortars (groups BO6-BO10-BO11 and BHP6-BHP10-BHP11) with that of concretes shows that the average value of the Herschel-Bulkley coefficient *b* for the mortars is 1.45. This is of similar in magnitude to that of the concretes, whereas the mortars are generally much less sensitive to segregation because of the limited size of the coarse aggregate and the increased importance of the surface forces with respect to the volume forces in the relative movements of the particles.

Therefore, we conclude that the rheological behavior of the mixtures that were studied is nonlinear, with some exceptions.

3.2.2. Suitability of the Bingham model for fresh concrete

An unexpected result of the present study consists in the need to provide at least *three* parameters to describe the rheological behavior of the fresh concrete: a significant complicating factor due to the fact that only one parameter, the slump, is currently used by engineers. The concrete community is reluctant to adopt the Bingham approach, itself more complex than the usual approach, according to which a single subjective property called "workability" is used to describe the flow behavior of fresh concrete. To what extent is the additional sophistication inherent in the Herschel-Bulkley model necessary? If one wishes to characterize the behavior of the concrete in a shear strain rate range from 0 to 6 s^{-1}, which encompasses the range of the rheometer, one may consider that the Bingham model is still sufficient, even if the method of calculating the yield stress and plastic viscosity parameters has to be changed. In fact, it is sufficient for this purpose to use a linear approximation of the Herschel-Bulkley curve in the shear strain rate domain in question. As to the plastic viscosity, the following equation can be established by minimizing the deviation between the two models (using the least-squares method):

$$\mu' = \frac{3a}{b+2}\dot{\gamma}_{\max}^{b-1} \qquad (5)$$

where μ' is the slope of this straight line (Figure 10) and $\dot{\gamma}_{\max}$ is the maximum shear strain rate achieved in the test. The yield stress, τ_0, is equal to the yield stress, τ_0', as calculated by the Herschel-Bulkley equation. The Bingham model with τ_0 and μ as values of the yield stress and of the plastic viscosity makes it possible then to maintain a relatively simple approach to the behavior, without having the disadvantage of a negative yield stress being calculated by Tattersall's original approach. The values of μ' were calculated for the concretes that were tested in the present project (Appendix IV to VI). The parameters μ and μ' are of the same order of magnitude, the latter being a little smaller when the value of the exponent b is greater than 1 (which is true in most of the cases).

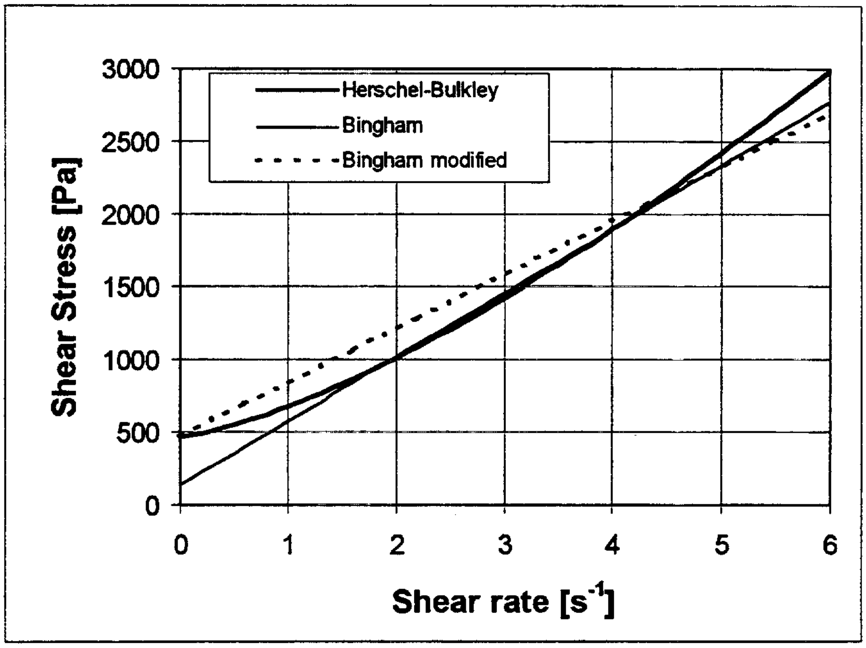

Figure 10. Calculation of the Bingham parameters based on the Herschel-Bulkley model. The dotted straight line departs from the same point as the HB model (abscissa 0, ordinate τ'_0).

This approach, using τ'_0 and μ' instead of τ_0 and μ, might not be suitable to represent the material rheological behavior in the case of shear strain rates larger than the range of measurement performed with the rheometer because the linear regression leads to larger errors in the range of shear rates higher than the region tested (Figure 10); or otherwise stated, because the modified Bingham model would not be able to represent the non-linear behavior at the large strain rates. For instance, in the case of pumping concrete, it may be necessary to use the original equation with all three parameters of the Herschel-Bulkley model.

Analysis of the collected rheological data, was used in the establishment of models linking rheological behavior with mixture composition. The results are given in the next chapter.

4. RELATIONSHIPS BETWEEN COMPOSITION AND RHEOLOGICAL PARAMETERS

4.1. A physical interpretation of the Bingham model

Fresh concrete is analyzed as a granular mixture (considering the entire population of particles, from cement to silica fume to gravel) in a water suspension. In this analysis, the content of entrapped air will be ignored. The minimum volume of water is that which corresponds to the porosity of the dry system. A concrete with zero workability is therefore, by definition, a packing in which the porosity is just saturated with water (Figure 11).

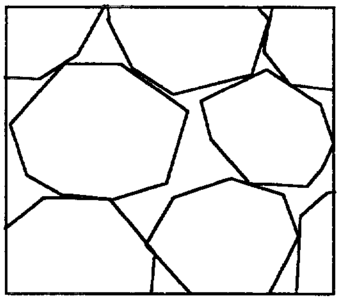

Figure 11. Suspension with minimum water content. No shearing movement is possible without localized rupture of the particule structure

4.1.1. The case of a mixture with single-size particles, i.e., with one granular class

An increase in the water content, beyond the minimum to fill the pores makes possible a water-filled spacing between the particles in the mixture, and, consequently, sliding between particles can be initiated (see Figure 12). If the shearing of the system is confined, a deformation will appear if this applied shear stress is sufficient to counteract the friction forces between the solid particles. Thus, the yield stress will be governed not by the liquid phase, the only role of which is to define the average distance between particles, but by the number and nature of the contacts between particles. Hence, for a mixture with a single size class of particles, there will be a relationship between yield stress and packing of the following form:

$$\tau_0 = f\left(\frac{\Phi}{\Phi^*}\right) \qquad (6)$$

where Φ is the volumetric fraction of solid material (with respect to a total volume of one), Φ^* is the maximum value of Φ for close packing (or the packing density of the dry mixture) and f is an increasing function. The ratio Φ/Φ^* is an expression of the relative concentration of solids, compared to the maximum packing. The function f increases with Φ/Φ^*, because the yield stress increases with increasing values of Φ/Φ^*.

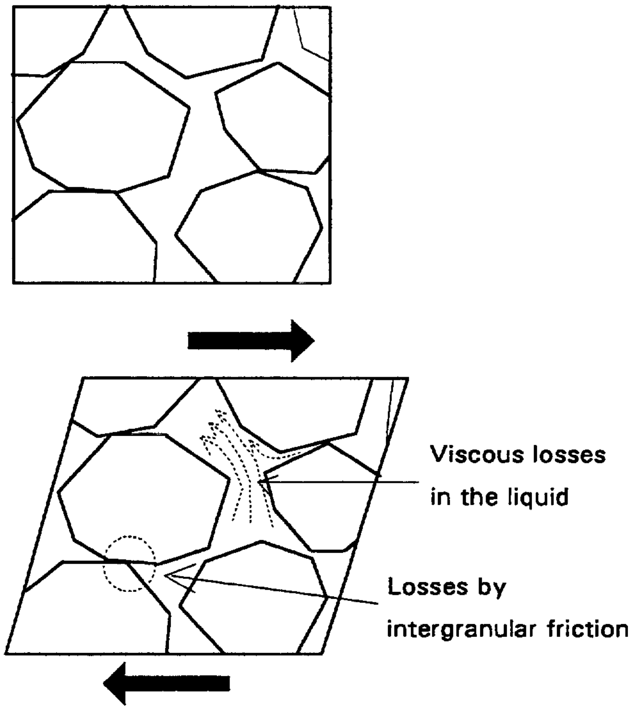

Figure 12. Suspension containing an excess of liquid compared with the minimum content

To investigate the microstructure of the flowing material, we will assume that the speed of each particle is equal to the macroscopic speed of the homogenized fluid, i.e., fresh concrete. Then, if the fluid remains in the laminar regime while flowing between the solid particles, its contribution to the shear resistance will remain proportional to the overall strain gradient.
Thus, in the classic form of the Bingham model:

$$\tau = \tau_0 + \mu\,\dot{\gamma} \tag{7}$$

where the term τ_0 is the contribution of the skeleton and the term $\mu\,\dot{\gamma}$ is the contribution of the suspending liquid. Based on the preceding analysis, a general form for the plastic viscosity, μ, can be deduced:

$$\mu = \mu_0\, g\left(\frac{\Phi}{\Phi^*}\right) \tag{8}$$

where μ_0 is the plastic viscosity of the suspending fluid and g is an increasing function of Φ/Φ^*. The function g is increasing because the plastic viscosity increases with the increase of Φ/Φ^*. A further explanation of this statement will be given in section 4.3.2.

4.1.2. Mixtures with several classes of particles

In the case of particles of several sizes, the value of the function *f* should depend on all the contributions of the various size classes of particles. Therefore the yield stress is as follows:

$$\tau_0 = f\left(\frac{\Phi_1}{\Phi_1 *}, \frac{\Phi_2}{\Phi_2 *}, \ldots \frac{\Phi_n}{\Phi_n *}\right) \tag{9}$$

where Φ_i is the volume fraction of granular size class i and Φ_i* is its maximum value for close packing, all of the other Φ_j $(j \neq i)$ being constant.

When the size and surface roughness of the particles change, the number of contacts between particles and the roughness of the particles change. It is therefore to be expected that the contribution of each size class to the yield stress includes size and roughness parameters relative to the particle fraction.

As to the plastic viscosity, it is already known, in the case of suspensions of single-size spheres, that the plastic viscosity does not depend on the size of the particles [25]. For binary systems of spheres, it appears that the parameter $\Phi/\Phi*$ continues to control the apparent viscosity, the influence of the size distribution being contained in the packing density term $\Phi*$ [26]. Clearly, it would be desirable if this assertion were to remain valid for particle systems with a large range of sizes in which the particles are not spherical. Thus, as a first step, an attempt was made to verify this assumption for the mortars and concretes that were tested.

If we refer now to the Herschel-Bulkley model, which was shown in 3.1.4 to be more applicable than the Bingham model for describing the rheology of fresh concrete, there is the question: "What is the physical origin for its mathematical form?" It can be inferred that the exponent of the relationship only reflects the increase (or reduction) in the plastic viscosity as the shear strain rate increases. The basic assumption that permits us to explain the Bingham model physically, i.e., the plastic viscosity does not depend on the shear strain rate, is probably true only for a narrow range of shear strain rates. Flocculation of particles, or the appearance of local turbulence, probably modify the flow conditions of the liquid phase in the interstices of the granular phase. Moreover, it is in the mixtures without HRWRA that, on the average, the strongest non-linearities have been found (i.e., the greatest values of the coefficient *b* in the Herschel-Bulkley model). It is also in these mixtures that the forces between fine particles are the most important, because the cement particles are not dispersed by the HRWRAs.

4.2. Calculation of the packing density of the mixtures tested

It follows from the previous considerations that the calculation (or measurement) of the packing density of the dry mixtures, defined as the maximum concentration (by volume) that the "dried out" suspension could attain, constitutes an essential preliminary step to modeling the rheological properties. A recent model developed for mathematically describing compaction of powders is described in the following section.

4.2.1. The compressible packing model

LCPC has been conducting studies for several years to develop models to predict the packing density of granular mixtures. A linear model for the packing density of particles mixtures was first developed [27], followed more recently by the Solid Suspension Model [28, 29], incorporated in the RENÉ-LCPC software [13]. The essential innovation in this second model consisted in distinguishing the *actual packing density* of a mixture, which was attained by using a given placement and compaction procedure, from the *virtual packing density*, the maximum packing density that could be attained only by putting the particles in place one by one. The virtual packing density was calculated as follows:

$$\begin{array}{l} \gamma = Min(\gamma_i) \\ 1 \le i \le n, \gamma_i \ne 0 \end{array} \qquad \textit{(Min = minimum value of } \gamma_i\textit{)} \qquad (10)$$

$$\gamma_i = \frac{\beta_i}{1 - \sum_{j=1}^{i-1} \left[1 - \beta_i + b_{ji}\beta_i(1 - 1/\beta_j)\right] y_j - \sum_{j=i+1}^{n} \left[1 - a_{ij}\beta_i / \beta_j\right] y_j} \qquad (11)$$

in which y_j is the proportion by volume of size class *i*, i.e., the ratio of the volume of size class *i* to the total solid volume; β_i is the virtual packing density of the *i*-class compacted alone; γ_i is the virtual packing density of the mixture when class *i* is *dominant* (i.e., when it is responsible for the "blockage" of the mixture); and the parameters a_{ij} and b_{ji} are *interaction coefficients* describing the "loosening" of the particles and wall effects, respectively. The loosening and wall effect can be defined as follows. In the vicinity of an isolated coarse grain, the packing of a small grain is disturbed. This effect is called the wall effect. Conversely, when an isolated fine grain is introduced in an interstice of a coarse grain packing, the coarse grain arrangement is disrupted. This second effect is called loosening effect [33].

In this model, using the γ_i parameters, a reference plastic viscosity could be calculated. This plastic viscosity depends on the placement method and the mixture composition. By analyzing a large number of test data (original tests or measurements taken from the literature [30, 31]), it was possible to tabulate reference viscosities against the placement method. Finally, the model provides an equation, which when solved numerically gives the theoretical value for the packing density. At the time the "Solid Suspension Model" was constructed, an empirical determination was made of the coefficients *a* and *b* (by smoothing the experimental values, which are presumed to be a function of the ratio between particle sizes). By calculating the β_i parameters for the packing density measurements related to a narrow range of the constituents, it was possible to calculate the theoretical packing density of each combination of these components. During validation studies, it was shown that an average error of less than one percent resulted when the model was used for predicting the packing density of the dry mixtures. It was also anticipated that the model would be equally suitable for predicting the plastic viscosity of the concentrated suspensions.

Subsequent evaluation of the model disclosed that:

- The fitting that leads to the interaction equations could be improved [32];
- The predictions of the plastic viscosity of binary sphere suspensions compared with experimental values taken from the literature [26] proved to be disappointing; and
- An error appeared in the calculation of the plastic viscosity with regard to a mixture of several granular size classes.

Consideration of these findings lead to the definition of a new model, called the *Compressible Packing Model* [33]. In this model, the hypothesis that led to the definitions of the virtual packing density values are preserved. However, the empirical expressions that predict the values of the interaction coefficients have been modified. The new expressions provide for better fitting of the experimental data and satisfy certain continuity conditions that were not taken into consideration before. These coefficients are as follows:

$$\begin{aligned} a_{ij} &= \sqrt{1-(1-d_j/d_i)^{1.02}} \quad && \textit{when } d_j \le d_i \\ b_{ij} &= 1-(1-d_i/d_j)^{1.50} \quad && \textit{when } d_i \le d_j \end{aligned} \qquad (12)$$

where d_i and d_j are the diameters of the granular classes i and j as defined by sieve sizes.

The concept of reference viscosity, which is difficult to justify physically, was replaced with the concept of a *compaction index K*. Like the reference viscosity in the previous model, this factor is assumed to be characteristic of the placement of the mixture. Thus, the emphasis is placed on the assumption that a granular packing is not a frozen structure, but may be considered as a compressible object, the state of compaction being described by the parameter *K*. Using considerations of the additive nature of particle contributions and of self-consistency, the following equation is proposed to define the compaction index:

$$K = \sum_{i=1}^{n} K_i = \sum_{i=1}^{n} \left(\frac{\dfrac{\Phi_i}{\Phi_i *}}{1 - \dfrac{\Phi_i}{\Phi_i *}} \right) = \sum_{i=1}^{n} \frac{y_i / \beta_i}{\dfrac{1}{\Phi *} - \dfrac{1}{\gamma_i}} \qquad (13)$$

where $\Phi*$ is the packing density of the granular mixture. The partial compaction indices K_i represent the contribution of each class to the overall index K. The values Φ_i* are the maximum values of the partial volume fraction Φ_i when packing is carried out (i.e., the maximum volume of particles i that can be placed in the mixture, the other values Φ_j, with $j \neq i$, remaining constant).

Compared with the solid suspension model, the improvement in predicting the experimental values of packing density is marginal [33]. Nevertheless, the compressible packing model better justified physically. The compaction index could thus be directly linked to the energy provided to pack the system. Typical values of the compaction index for various placement procedures for dry particles are given in Table 3. For the water-demand tests performed on mixtures of binders [34], a value 6.7 for the index K is found for this type of system (compaction of the fine particles in a very concentrated suspension under the effect of mixing and capillary forces) [35].

Table 3. Compaction indices for various procedures for preparing dry granular packings [33].

Placement	Simple pouring	Dry-rodding	Vibration	Vibration + Compression 10 kPa
K	4.1	4.5	4.75	9

4.2.2. Validation for several dry mixtures in the present program

Until now, attempts at direct validation of packing density models have only concerned granular materials of a smaller range of particle size than that of concrete [29]. It was, therefore, hoped that the applicability of the new model to cement-and-aggregate mixtures could be verified. We first measured the dry packing density of the cement, using the same procedure as used for the aggregates (see section 2.1.1) (the value derived was 0.553). Given the compacting process and the compaction index associated with it, the value of the virtual packing density is less than that of the cement in the presence of water (0.61 instead of 0.64). This shows that the forces of interaction between particles and the friction forces they generate are more significant in air than in water, despite the formation of hydrates, which occurs from the first contact between the water and the anhydrous cement. In other words, if the fresh concrete were dried out, e.g. by using a drained vibro-compaction procedure to squeeze out the maximum amount of the interstitial water, it will be expected to obtain a higher packing density than for the dry mixture.

The dry mixtures were then prepared using the same composition of dry ingredients (sand, coarse aggregates and cement) as selected mixtures, i.e., BO2, BO5, BO7 and BO11(Chapter 3) and their dry packing densities were measured. The agreement with the predictions of the compressible packing model was excellent (Figure 13), and confirms that the model is applicable throughout the range of particle sizes used in this study.

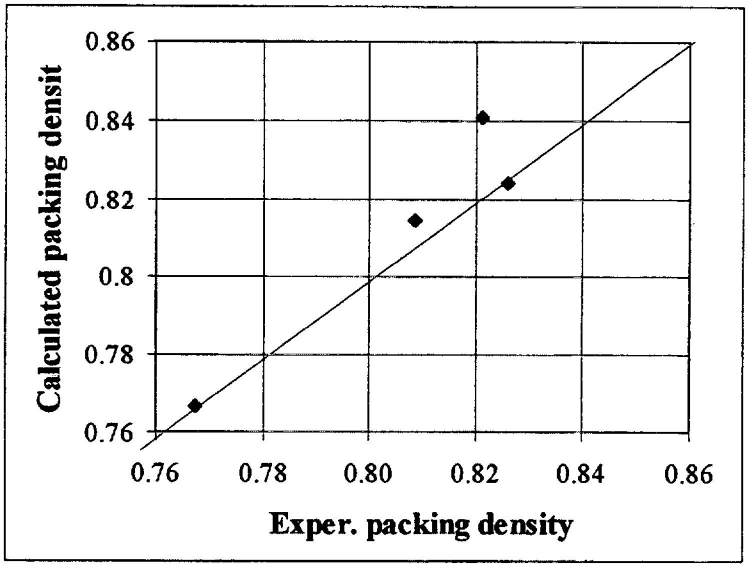

Figure 13. Comparison of the experimental values of packing density with the predictions of the Compressible Packing Model for dry cement-sand-gravel mixtures

4.2.3. Calculating the packing density of the wet mixtures

The effect of the presence of water on the virtual packing density of the cement shows that the parameters β_i needs to be calculated from measurements made on the binders in the presence of water. Recall that β_i is the virtual packing density of a single-size fraction [13]. Also, the experimental program includes intermediate mixtures with dosages of HRWRA between 0 and the maximum value (the saturation dosage). Therefore, the variation in the demand for water by the cement, as a function of the percentage of HRWRA, "SP%", has been systematically measured and the change in the packing density of the cement, c, (corresponding to a *K* value of 6.7) has been determined (Figure 14). This maximum packing density of the cement is effectively expressed by an empirical equation of the parabolic type:

$$c = 0.6065 - 0.047\,(1 - SP\%)^2 \qquad (14)$$

Using these estimated values of packing density, the values of the virtual packing density, β_i, for the cement with various doses of HRWRA were deduced (see Table 4). It was then possible to calculate the packing density, Φ^*, of each mixture group for a compaction index of 9. Based on our work with dry mixtures, a compaction index of 9 is characteristic of a highly compacted random packing. The values of Φ^* are given in Appendix VII.

Table 4. Values of the virtual packing density of the cement for different dosages of HRWRA

% by mass HRWRA/cement	0	0.2	0.4	0.6	0.8	1
Estimated packing density	0.559	0.576	0.590	0.599	0.605	0.606
Virtual Packing density, β_i	0.416	0.426	0.438	0.445	0.451	0.452

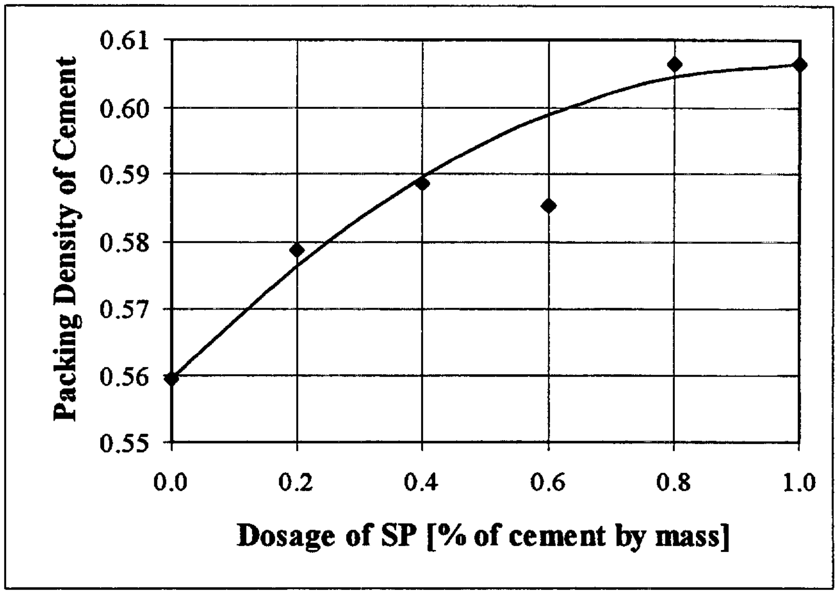

Figure 14. Packing density of the cement as a function of the dosage of HRWRA (SP) in the water-demand test.

4.3. Modeling the rheological parameters

4.3.1. Review of the existing models of plastic viscosity

Hu examined the literature concerning rheological models linking mixture composition and viscosity of suspensions [7]. He found that most authors [7, 36, 37, 38] analyzed fresh concrete as a paste/aggregate composite and tried to deduce the plastic viscosity of the concrete from the plastic viscosity of the paste by multiplying it by a function that took into account the volume and nature of the granular phase. Some authors even extended this analysis to the cement paste, using the Farris approach. In order to calculate the plastic viscosity of the multi-modal suspensions, they performed an iterative calculation, the whole being made up of the suspending fluid and the finest classes being dealt with homogeneously at the scale of a given class [25]. As elegant as they might be, these models suffer from not taking into consideration the inter-particle interactions. In fact, most concrete mixtures have a more or less continuous size distribution, so that the division into a number of discrete classes is arbitrary. Even the distinction between cement paste and aggregate, which is pertinent in the case of hardened concrete, is difficult to justify for fresh concrete. The large particles of cement are of comparable size to the finest sand particles and their respective contributions to the rheology of the whole are not of a different nature (at least as long as the hydration of the cement remains negligible). One way of attempting to link the rheology of the neat cement paste with that of concrete was to introduce another factor, i.e., the gap existing between the aggregates [39]. However, this approach requires measuring the rheological behavior of the paste through independent means, which was not done in the present study.

4.3.2. A simple model of plastic viscosity applicable to the six families of mixtures

The model described herein is based on the work of Chang and Powell, in which the relative concentrations of the suspensions were treated as controlling their plastic viscosity [26]. When the experimental plastic viscosity μ' measured in this study is plotted as a function of the ratio between solid volume fraction and packing density, the plot in Figure 15 is obtained. The solid volume fraction that is used that of the "de-aired" mixture, which means that the quantity of air has been disregarded (see Figure 16). This assumption is not entirely valid. In fact, it is known that mixtures consolidated by vibration always contain a certain volume of entrapped air, which varies from 1% for fluid concretes to 4% and more for mortars with HRWRA. Moreover, the plastic viscosity is measured for the sheared (and thus unconsolidated) mixtures, the air content of which is probably greater than that of unsheared or consolidated mixtures. However, this volume of air is difficult to measure (tests deal with consolidated concrete, while concrete under shear exhibits dilatancy) and in any case is governed by the rheology of the system, i.e., a given mixture increases its dilatancy with a decrease of water content. In the absence of reliable data on this subject, the volume of aggregate that would have been obtained after total consolidation was used.

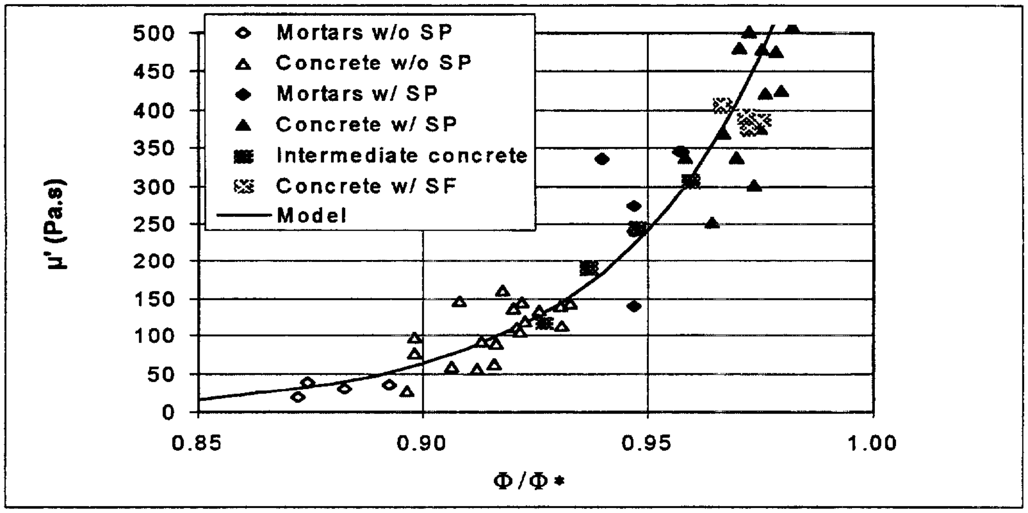

Figure 15. Plastic viscosity (μ') of the mortars and concretes as a function of their relative solid concentrations.

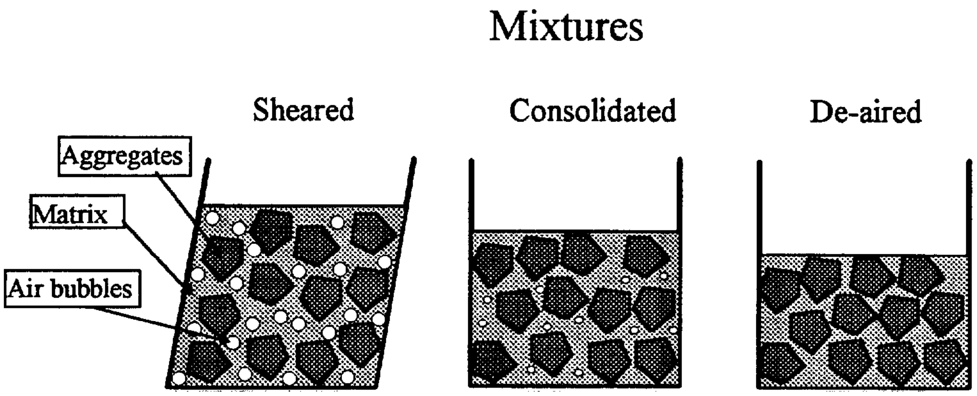

Figure 16. Different states of compaction of a wet mixture.

The relative concentration of solids has a significant effect on the plastic viscosity. It is quite remarkable that the experimental points in Figure 15 are grouped about a single curve, regardless of the nature of the mixture (mortars or concretes, with or without HRWRA, and with or without silica fume). An empirical equation for the best fit curve is:

$$\mu' = \exp\left[26.75\left(\frac{\Phi}{\Phi*} - 0.7448\right)\right] \qquad (15)$$

and provides an evaluation of the experimental plastic viscosity with an average relative error of 27%. The uncertainty concerning the packing density parameter Φ* (on the order of ±1% in terms of absolute value) explains part of the dispersion of the experimental points around the calculated curve. The volume fraction of solids is also subject to a certain error since the sheared mixture is less compacted than the consolidated mixture. Finally, the plastic viscosity μ', calculated from the Herschel-Bulkley parameters, valid for a limited range of the shear strain rate, also has an error, which is about 10% for the cohesive mixtures [7] and probably more for mixtures exhibiting bleeding and segregation. This is one reason that the present model does not appear to be easily improved by taking into account secondary parameters other than the fundamental parameter of relative solid volume concentration of solids.

According to this model, the effect of the HRWRA on the plastic viscosity is through deflocculation of the cement, which is expressed by a lower water demand and by a greater packing density, Φ*, of the mixtures.

4.3.3. A semi-empirical model for the yield stress

When the yield stress is plotted as a function of the relative concentration of solids (Figure 17), the same trend as observed for the plastic viscosity is not obtained. It appears that it is necessary to consider the contributions of the various granular fractions, according to the nature of the materials.

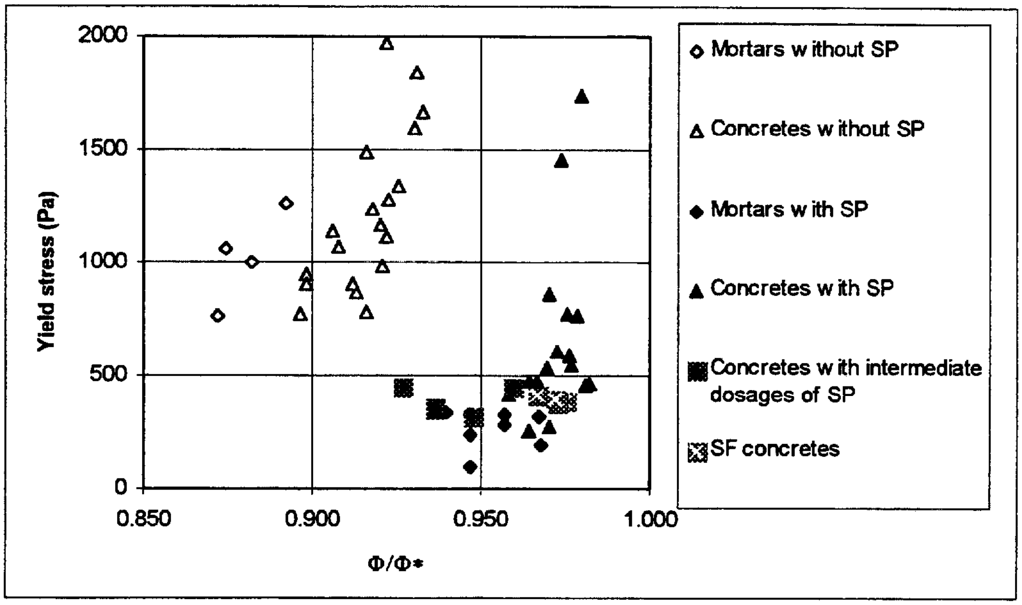

Figure 17: Yield stress as a function of relative concentration of solids

Returning to the formulation of the compaction index (equation 8), it is found that the form of this expression is similar to the equation type needed. The terms K_i are functions of the relative volume concentration of size class *i* (the terms Φ_i/Φ^*_i) and this type of expression is the only one that permits the terms to be additive and self-consistent [33]. It is thus tempting to develop models from linear combinations of the partial compaction indices K_i, since one can then sum the terms K_i relating to different fractions having a similar size composition (for example, the different fractions of sand, a material with a large grading span compared to the other components). However, in calculating the terms K_i, it is necessary to take into account the solid volume *in the de-aired concrete* (or in the mortar) and not in the corresponding dry mixture. In order to avoid this confusion, the compaction indices related to de-aired concrete will be called K'_i. They are calculated with a value for the parameter Φ equal to 1 minus the volume of free water (the difference between the total water in the mixture and the water absorbed by the aggregates). The following two equations have been obtained by a fit to minimize the absolute difference between the measured and calculated values. For mixtures without HRWRA we obtained:

$$\tau'_0 = \exp(2.537 + 0.540K'_g + 0.854K'_s + 1.134K'_c) \qquad (16)$$

and, for the mixtures with 1% HRWRA (without silica fume), we obtained:

$$\tau'_0 = \exp(2.537 + 0.540K'_g + 0.854K'_s + 0.224K'_c) \qquad (17)$$

In these equations, τ'_0 is the yield stress obtained by fitting of the rheometer results in accordance with the Herschel-Bulkley model. The indices *g*, *s* and *c* relate to gravel, sand and cement, respectively.

The average error of these models is 163 Pa (see Figure 18). The error is reduced to 109 Pa if we exclude from the set the mixtures BO4C, BHP4A and BHP4B. For these mixtures the model underestimates the yield stress, because their high gravel content and low cement content, promote segregation and aggregates interlocking.

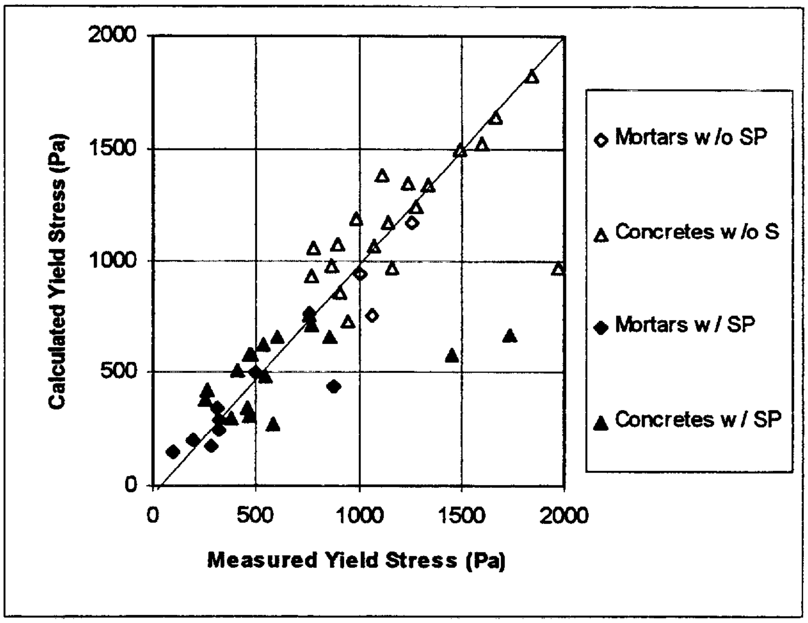

Figure 18. Comparison between experimental values and model values of the yield stress.

By comparison, the error due to the uncertainty regarding the friction of the rheometer joint is on the order of 60 Pa [8], to which must be added the repeatability error due to the sampling of the material, the value of which is on the order of 10% of the yield stress. Therefore, the precision of the model is felt to be satisfactory considering the experimental uncertainties. As to the number of adjustable parameters, it may appear high (five multiplier coefficients for the *K*'s factors), but it remains small compared with the number of experimental points used to determine the coefficients (49).

In the model given by equation 16, it is found that the multiplier coefficients of the partial compaction indices are ordered logically according to the particle size: they increase as the size decreases. However, this increase is not proportional to the specific surface area since the elementary friction due to contact between the particles probably decreases when the number of contacts per unit volume increases. This may be why all of the approaches based on taking the specific area of the aggregates as a fundamental parameter for the rheology have always failed or required empirical correction [40].

In the second model represented by equation 17, the contribution of the aggregates is unchanged while the cement contribution is strongly reduced. It is thus seen that the introduction of the HRWRA into the mixture has two effects. In the first, the HRWRA increased the deflocculation of the cement, which permits the fine particles to pack more efficiently in the interstices between the large particles, reducing the water demand. In the second, the organic molecules are adsorbed onto the solid surfaces and lubricate the contacts between particles. This lubrication reduces the shear stresses at the contact zones, explaining the reduction of the coefficient of K'_c by a factor of 5. In mixtures with high dosages of HRWRAs, it is the granular skeleton that is mostly responsible for the yield stress. This is why the yield stress is directly linked to the relative concentration of aggregates (Figure 19).

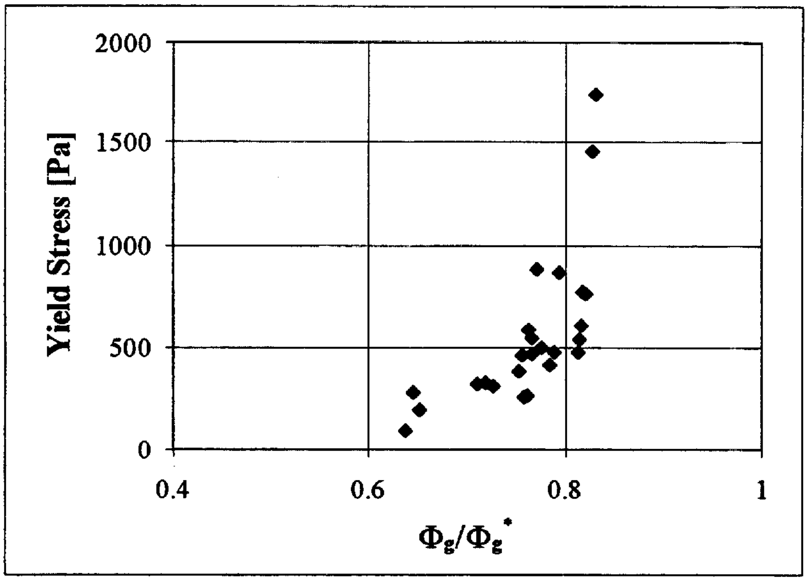

Figure 19. Relationship between the experimental yield stress and the relative concentration of the aggregate (g/g*), for mixtures with HRWRA.

4.3.4. The case of concretes with silica fume

As described in section 2.3.4, four silica-fume concretes were generated from the *central* mixture with HRWRA. Increasing percentages of silica fume were added while the solid-volume proportion of cement was kept constant, and the water was adjusted to remain in the region of measurable flow. The dosage of HRWRA was increased to maintain a condition of maximum deflocculation of the fine particles. The reduction in the water dosage did not compensate for the addition of silica fume, so that the volume of paste continuously increased. The yield stress does not continuously decrease with silica fume dosages varying between 0 and 30% of the mass of cement. A minimum is reached at around 15% silica-fume (at the limit of significance), while the yield stress clearly increases for greater dosages of silica fume (see Figure 20). Thus, it appears that the silica fume has a specific effect on the yield stress, even in the presence of HRWRA. In order to evaluate the multiplier coefficient of the term K'_{sf} added to equation 17, we first searched for a value that would produce a theoretical curve (yield stress, dosage of silica fume) that was approximately parallel to the experimental curve. This condition is satisfied for an fitted value of 1.5 (Figure 20). If a simple statistical approach to minimize the deviation between the model estimates and the experimental values on all four silica-fume concretes is pursued, a value on the

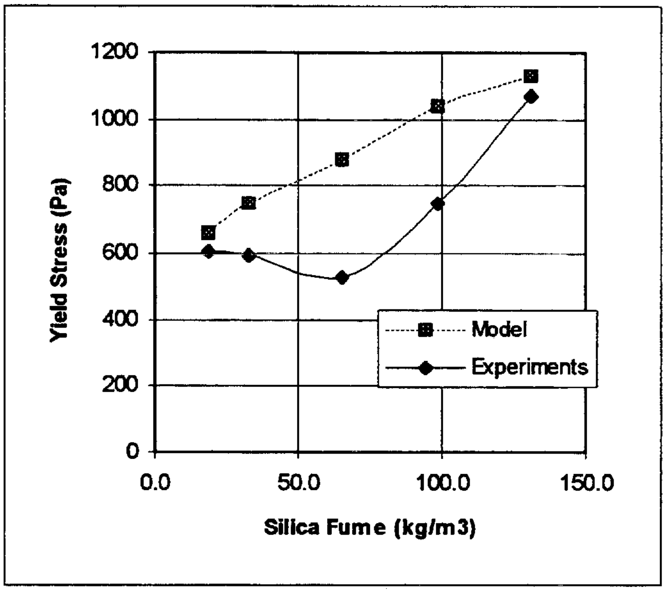

Figure 20. Relationship between the yield stress and the silica fume content. $K'_{fs} = 1.5$.

order of 0.806 is obtained for the K'_{sf} coefficient. Additional studies are needed to choose between these two options.

Nevertheless, it appears that the contribution of the finer material (diameter less than 80 μm) to the yield stress in the presence of HRWRA is not a function of their size alone. The affinity of the surfaces to the polymer appears to play a role. In addition, it is known that silica fume adsorbs the naphthalene sulfonates because of its silanol groups [41]. However, the quantity adsorbed per unit of surface area is probably less than that of the portland cement, and hence the effectiveness of the HRWRAs in reducing the shear stress would probably be less.

The results obtained in this study were also used for our third goal, i.e., to develop a simple and cheap field test. We will describe the test and use the same data as in the rheology study to validate the use of the new device, which is a modification of the standard slump test.

5. THE MODIFIED SLUMP TEST

5.1. Background

While laboratory rheometers provide comprehensive data, present field methods are severely limited because most of time they give only a value related to either yield stress or plastic viscosity. Laboratory rheometers are sophisticated and expensive, while most field test are easy to use and inexpensive. Due to the variability of the composition of the components and the difficulties in determining the proper water dosage, concrete mixtures are typically not optimized for performance. To optimize concrete for performance and to improve the uniformity of the material's most important properties (including the rheological properties), rigorous quality control with the possibility of correcting in real time, as needed, is paramount. The measurement of rheological properties of concrete is straightforward in the laboratory using a rheometer of the type described in this report but it must be used by trained personnel and the device is expensive. Therefore, there is a need for a simpler, inexpensive device for making rapid and reliable measurements in the field.

Even if the rheological behavior of the concrete is reduced to two parameters (yield stress and plastic viscosity), the array of current rheological tests for field use does not permit them to be evaluated, except very roughly. While the slump test, the grandfather, and most widely used, of all tests, provides an indication that is reasonably well correlated to the yield stress [7], the other tests — DIN flow table, VEBE apparatus, etc. [42] — provide results that are not very useful in terms of characterizing the rheological parameters. In most of these tests, the concrete flows under the effect of a dynamic loading. Thus, the behavior of the concrete under vibration is brought into play, although nothing indicates that this is related directly to the behavior of the unvibrated concrete (as illustrated by the Bingham parameters).

A survey of the state of the art showed that none of the current "field" tests (in distinction to rheometers) makes it possible to assess the plastic viscosity of the concrete [42]. However, this parameter is assuming increasing importance in modern concretes. For high-performance concretes, it frequently constitutes *the* critical parameter that controls pumpability [7], and ease of finishing. This chapter describes a modification of the slump apparatus that, on the basis of the measurement of a partial slump time, makes it possible to evaluate the yield stress **and** the plastic viscosity in the field.

5.1.1. Previous work of Tanigawa et al. [9,10]

Professor Tanigawa's team in Japan has played a large role in development of the applications of the rheology of fresh concrete. In particular, these researchers have performed finite-element analyses of the current rheological tests to establish equivalencies between the results of these tests and the fundamental rheological properties [9]. However, for lack of a concrete rheometer, it was not possible to validate most of their calculations by test results, which limits their application and is a possible reason why Japan, although very active in research on the properties of fresh concrete, has not yet routinely utilized the concepts of rheology in industrial practice (to the authors' knowledge).

Concerning the standard slump cone test, Tanigawa et al. [9;10] performed measurements of the slump as a function of time (Figure 21). They found that the slump-time curve could be simulated by finite element analysis of the fresh concrete assuming it to be a Bingham material. The slump-time curve depends on both the yield stress and the plastic viscosity. Since the final slump is related directly to the yield stress, it is reasonable to assume that the time-dependence of slump is likely to be controlled by the plastic viscosity. Considering that the slump test is currently the only field test in the world for most practitioners, the apparatus was modified slightly in this study in an attempt to measure both the yield stress and the plastic viscosity of fresh concrete. This chapter describes the modification made to the standard slump test apparatus, test procedure and calculation to determine both the yield stress and the plastic viscosity.

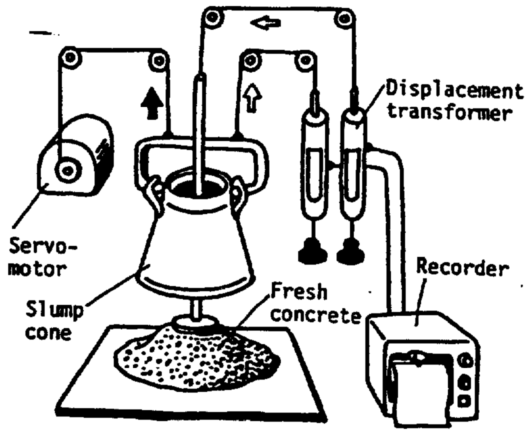

Figure 21. Experimental setup of Tanigawa et al. [9, 10] for recording the slump as a function of time.

5.1.2. Design and dimensions of the modified slump test apparatus

Since the goal was to develop a test that was above all simple, robust and inexpensive, it was not practical to record the slump as a function of time. To do a complete recording, it would have been necessary to provide for electronic data acquisition. The interpretation of the resulting curve would also have been too complex. Therefore, it was decided to try to characterize the plastic viscosity based on an average rate of slumping in the slump test. Thus, measurement of the time necessary to reach an intermediate height between the initial and final values appeared *a priori* to be a good means of discriminating among the concretes according to their plastic viscosity.

The choice of this "partial slump" took into consideration two potential problems: (1) a height that was too small would lead to very small slump times and thus poor relative precision of measurement; (2) a partial slump that was too large would rule out all of the concretes with a smaller final slump. Since the range of concretes that can be characterized by the rheometer is, as already stated, approximately that for which the slump is greater than 100 mm, this value was chosen for the partial slump.

The Tanigawa setup for measuring slump as a function of time would be too fragile for a work-site environment [9]. Therefore, we adopted the use of a plate, allowed to slide on a centrally-located rod as the means for monitoring the time to reach the 100-mm slump. The rod coincides with the axis of symmetry of the conic frustum. Since the axis of symmetry was in principle preserved during the flow of the concrete, the rod would not be expected to greatly disturb the slump. This point was later verified.

In order to measure the partial slump time, it was adequate to use a stopwatch controlled by the operator on the basis of a visual criterion (such as in the VEBE test). The stopwatch is started at the beginning of raising of the cone, and is stopped when the sliding plate placed on the fresh concrete reaches the stop on the rod (Figure 22). The dimensions of the apparatus and the test setup are shown in Figure 23 and Figure 24.

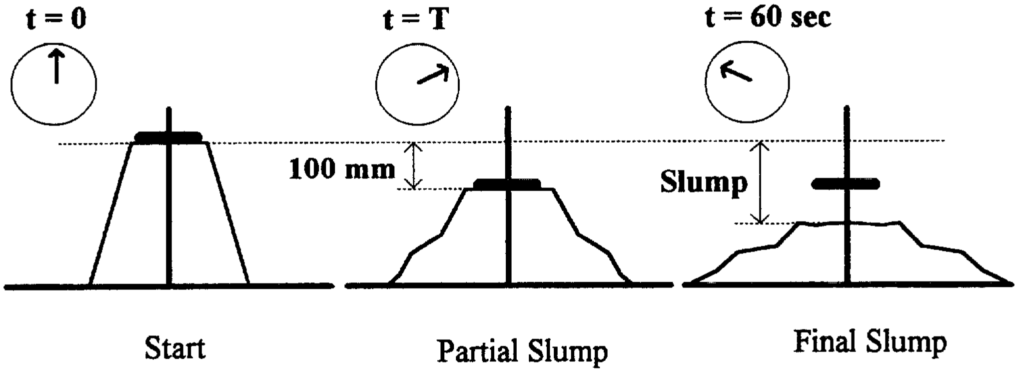

Figure 22. Schematics of the modified slump cone test. T is the "slump time".

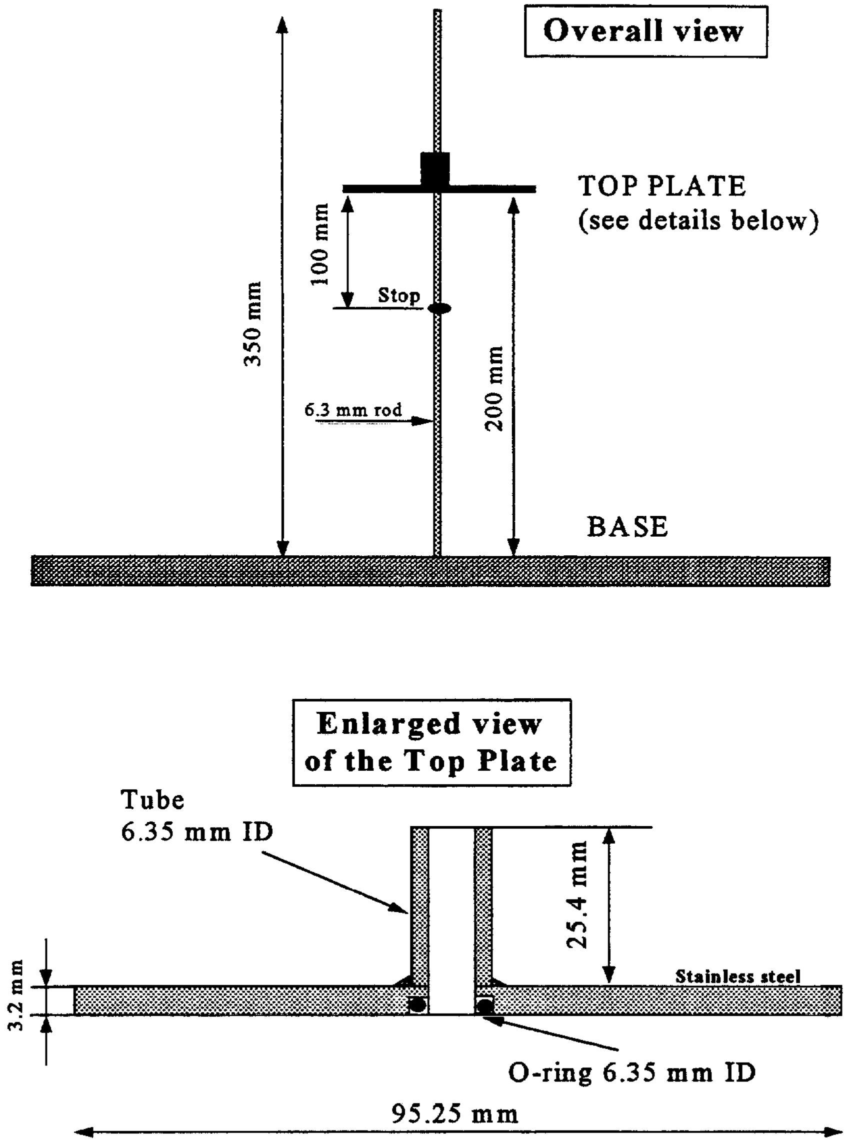

Figure 23. Rod and top plate in the modified slump apparatus.

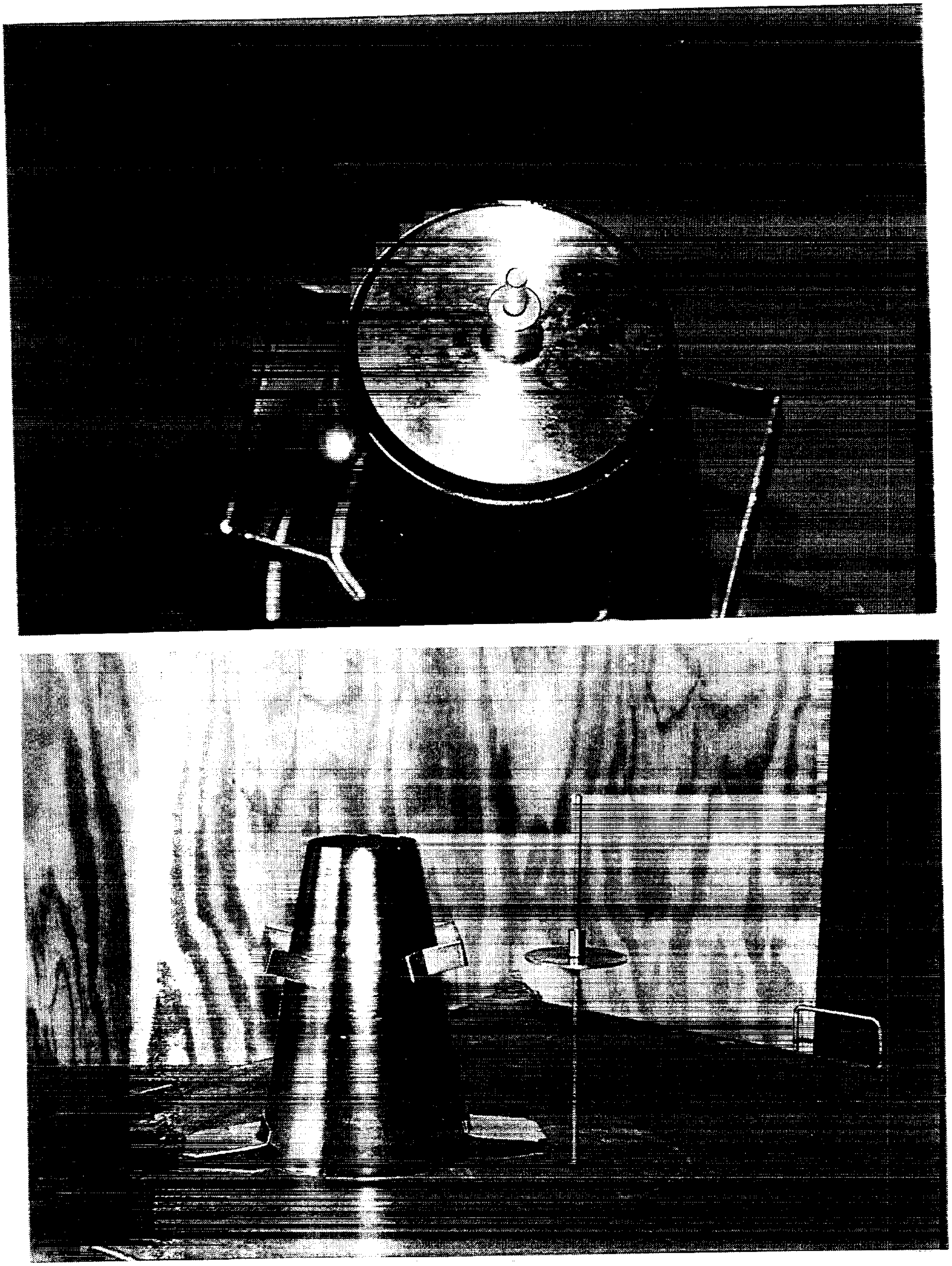

Figure 24. The modified slump test apparatus: A) View from above the mold showing the top plate; B) View of the mold, the rod attached to the base and the top plate at the final position.

5.2. Measurement of the slump time

5.2.1. Procedure for measuring the slump time

The following components are needed to conduct the modified slump test:

- A horizontal base to which the rod is attached;
- A standard mold for the slump test (ASTM C143 [17]);
- A sliding disk (the upper plate);
- A rubber o-ring seal, the purpose of which is to prevent fine materials from interfering with the fall of the disk;
- A rod to consolidate the concrete;
- A small trowel to finish the upper surface of the concrete;
- A ruler to measure the slump;
- A stopwatch with a resolution of 0.01 s.

The concrete was placed in the same manner as in the standard slump test (ASTM C143-90 [17]). The various stages are as follows:

1. Carefully clean the rod and coat it with grease or petroleum jelly (down to the stop);
2. Using a wet sponge, moisten the base and the inside wall of the mold;
3. Place the mold on the base, assuring that the rod is centered with respect to the upper opening;
4. While keeping the mold in place on the base (either with attachments provided for this purpose or by standing on the foot pieces welded to the outside of the mold), fill it in three layers of equal volume, rod each layer 25 times;
5. Strike off the surface of the concrete, assuring that it is level as possible with the top of the mold;
6. Using a rag, clean the part of the rod that projects above the concrete specimen;
7. Slide the disk along the rod until contact is made with the surface of the concrete;
8. Raise the mold vertically while starting the stopwatch;
9. While the concrete is slumping, *continually* observe the disk (through the top of the mold) and stop the stopwatch as soon as the disk stops moving;
10. Once the slump has stabilized, or no later than one minute after the start of the test, remove the disk and measure the slump with the ruler.

5.2.2. Measurements made on 78 mixtures

The modified slump test as described was performed on all of the mixtures and the partial slump times (which will hereafter be called the slump times) are given in the tables in Appendix IV-VI. When the mortars and concretes for which the final slump was less than 100 mm are excluded, the measured slump times range from 0.63 seconds to 15.97 seconds.

One question was whether the minimum time was controlled by the slump of the concrete, with the disk remaining in contact with the concrete during the fall. The theoretical time for an initially stationary body subject to gravity to free fall a distance h of 100 mm is $\sqrt{2h/g}$, or 0.14 seconds. Two measurements of the fall time of the disk on the rod (without concrete) gave values of 0.16 seconds and 0.15 seconds. Hence, it was concluded that any separation from the concrete was unlikely (at least with the concretes tested). In addition, the precision of measurement is on the order of 1/10 of a second due to the reaction times of the operator. Also, the variability will be larger because the cone lifting is not precisely controlled [43].

The consistency of the measurements was examined by considering the variation in slump time within each mixture group. With rare exceptions, the times are on a single curve when plotted against the volume of mixing water: they decrease regularly as the water dosage increases. On the other hand, comparison of the average values of series of measurements is equally instructive and encouraging. The average slump times of all mixtures without HRWRA is 1.51 seconds (range ± 0.54 seconds), while the values for mixtures with HRWRA are generally greater and more widely spread (average of 4.80 seconds, range of ± 4.66 seconds). Therefore, this test will be more useful in determining the plastic viscosities of concretes with HRWRAs.

5.2.3. Comparison of final slumps obtained with the standard test and the modified test

A check was done to determine whether the modification to the standard slump test affected the final slump measurement. This was necessary to have complete compatibility with the unmodified test.

The mass of the disk (212 g) increases the vertical stress on the sample by a maximum value equal to its weight divided by the upper area of the frustum, i.e., 0.27 kPa. When the disk reaches the stop, the height h of the concrete is 200 mm. Hence, the vertical compression stress at the base of the sample equals ρgh (where $\rho = 2400$ kg/m^3 is the approximate density of the fresh concrete and g is the acceleration due to gravity), i.e., about 4.8 kPa. It is thus seen that the vertical stress due to the disk is at most on the order of 6% of the stress due to the concrete. The friction of the concrete along the rod would tend to reduce the final slump. To verify that the effects of the disk and the rod are negligible, a comparative study was done with six compositions chosen to be representative of the range of slumps obtained. The two tests (the standard slump test and the modified test) were conducted in parallel. Figure 25 shows the comparison between the two tests. The best fit line with an intercept of 0 has a slope of 1.01 with a standard error of 0.03. The residual standard deviation of the line is 17 mm. Therefore, the slumps measured with the two tests are identical.

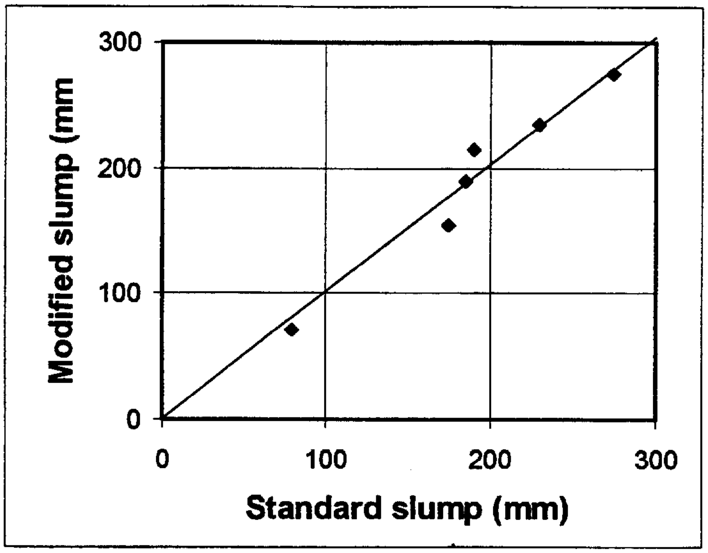

Figure 25. Comparison of the slump values between the standard slump test and the modified test.

5.3. *Estimation of the fundamental rheological parameters on the basis of the modified slump test*

5.3.1. Models to evaluate yield stress

Based on finite element analysis of the slump test and on measurements of the yield stress using the rheometer and of the slump, Hu proposed a general formula relating the slump *s* to the yield stress τ_0 [8] in the following form:

$$\tau_0 = \frac{\rho}{270}(300 - s) \tag{18}$$

where ρ (density) is expressed in kg/m³, τ_0 in Pa, and *s* in mm. A correlation with experimental data was shown to give a reasonable prediction of the Bingham yield stress. However, despite the fact that the plastic viscosity is not taken into account in equation (2), it does play a role. Hu found that the correlation is poor if the concrete's plastic viscosity is greater than 300 Pa·s. Figure 26 compares the experimental yield stress obtained from the Herschel-Bulkley model with the estimated yield stress based on equation (18).

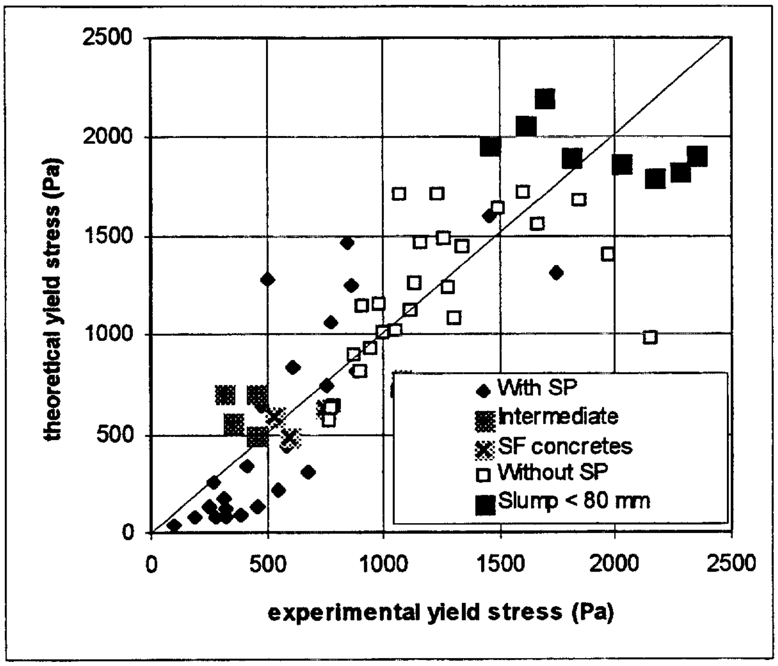

Figure 26. Comparison between the experimental yield stresss from fitting the Herschel-Bulkley model and predictions from Hu's model (equation 18) [7]. The line represent the perfect correlation (45 ° line).

The predictions for the yield stress provided by this model are quite reasonable. There is an average error of 195 Pa for the yield stress in the range of 100 to 2000 Pa. (Figure 26). However, there is a systematic underestimate of the yield stress in the low range, typical of self-leveling concretes. The accuracy of Hu's model can be improved empirically by adding a constant term and modifying the slope term. The following equation:

$$\tau_0 = \frac{\rho}{347}(300 - S) + 212 \qquad (19)$$

results in a 162 Pa average error with respect to the measurements (see Figure 27). The improvement is particularly notable for the very fluid mixtures.

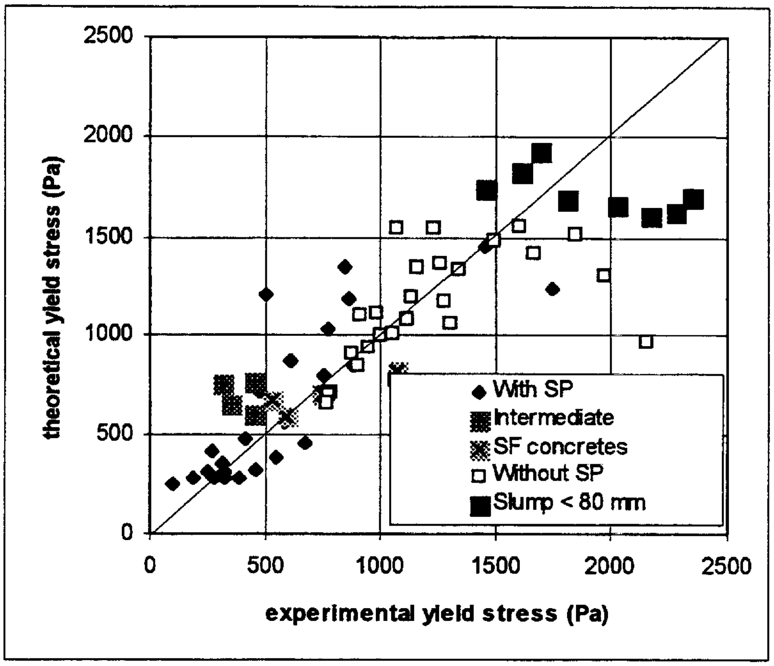

Figure 27. Comparison between experimental yield stress from fittingthe Herschel-Bulkley model and predictions using equation 19. The line represent the perfect correlation (45 ° line).

5.3.2. A semiempirical model for evaluation of the plastic viscosity

To evaluate the plastic viscosity from the results of the modified slump test, the following assumption was invoked: for concretes with the same final slump and the same density concrete, a difference in slump time can be attributed to a difference in plastic viscosity. From a dimensional analysis, it can be expected that the factor $\mu/\rho g T$ (where μ is the plastic viscosity and T the slump time) is a function of the final slump. Figure 28 shows the value of the factor $\mu/\rho T$ plotted as a function of slump for the mixtures with slump less than 260 mm. For the mixtures with higher slumps (self-leveling concretes), the scatter is larger because of the very short slump times and the higher probability of segregation.

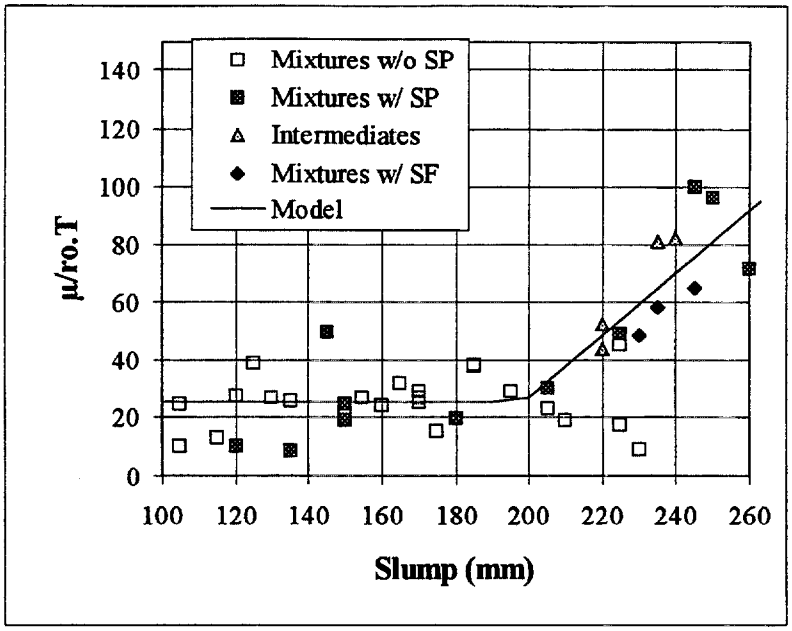

Figure 28. Relationship between the ratio µ/ρT and the final slump

If we consider only the concretes having a slump less than 260 mm, the best fit to the data is given by the following equations:

$$\mu = \rho T \bullet 1.08(s-175) \qquad \text{for } 200 < s < 260 \text{ mm}$$

$$\mu = 25\, \rho T \qquad \text{for } s < 200 \text{ mm} \qquad (20)$$

From these equations, the plastic viscosity can be estimated from the density, the final slump (in mm) and the slump time (in seconds). The average error for this model for all the concretes with a slump between 120 mm and 260 mm is 66 Pa·s (Figure 29). Two mixtures (BHP4C and BHP4B), that deviate significantly from the correlation, can be considered outliers because their composition included an excess of gravel (which is rare in practice especially for superplasticized concretes), and because there was a lack of cohesion during the slump tests. Excluding the two outliers, a linear correlation a slope of 1.09 ± 0.03 (Figure 29) is found between the theoretical and measured plastic viscosity. This slope indicates a very good correlation between the two entities.

To avoid calculations using equations 19 and 20, nomographs are given in Figure 30 to rapidly estimate the yield stress (in Pa) and the plastic viscosity (Pa·s) from measurements of the final slump and the slumping time with the modified slump test for a concrete with a density of 2400 kg/m^3.

In using these models and empirical equations to determine the yield stress and the plastic viscosity, we assumed that the concrete followed the modified Bingham model described in section 3.1.4.

In conclusion, the modified slump tests and model presented allows an evaluation of the plastic viscosity of concretes but with a lower accuracy than from the rheometer. Therefore, the modified slump test is most likely to be used as a quality control procedure in the field, and the rheometer as a development instrument for determining the optimum mix design for a specific application.

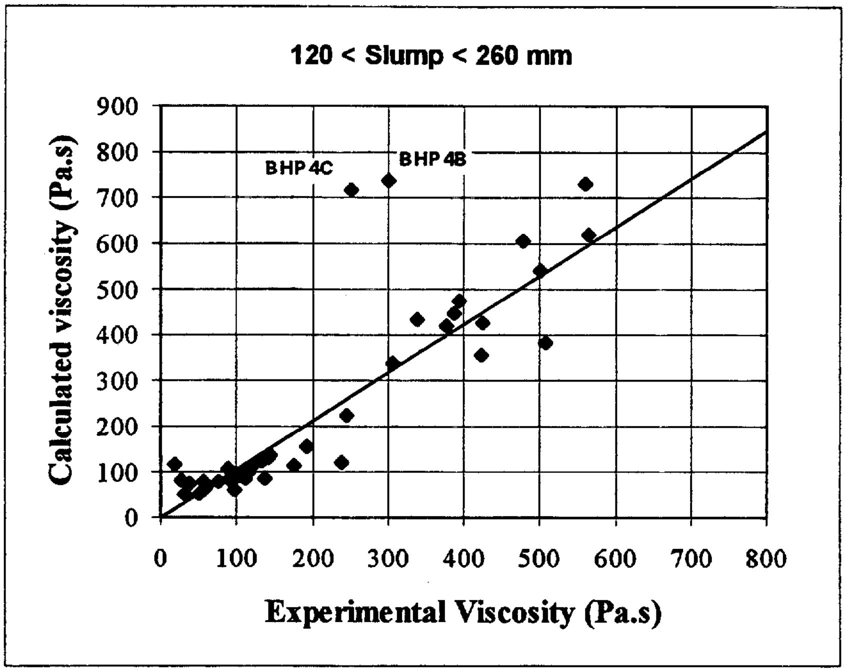

Figure 29. Comparison between measured plastic viscosity using the BTRHEOM and predictions from the plastic viscosity model (equation 20) for concretes with slumps between 120 mm and 260 mm. The slope of the best fit straight line, shown, passing through the origin is 1.09 with a standard error of 0.03.

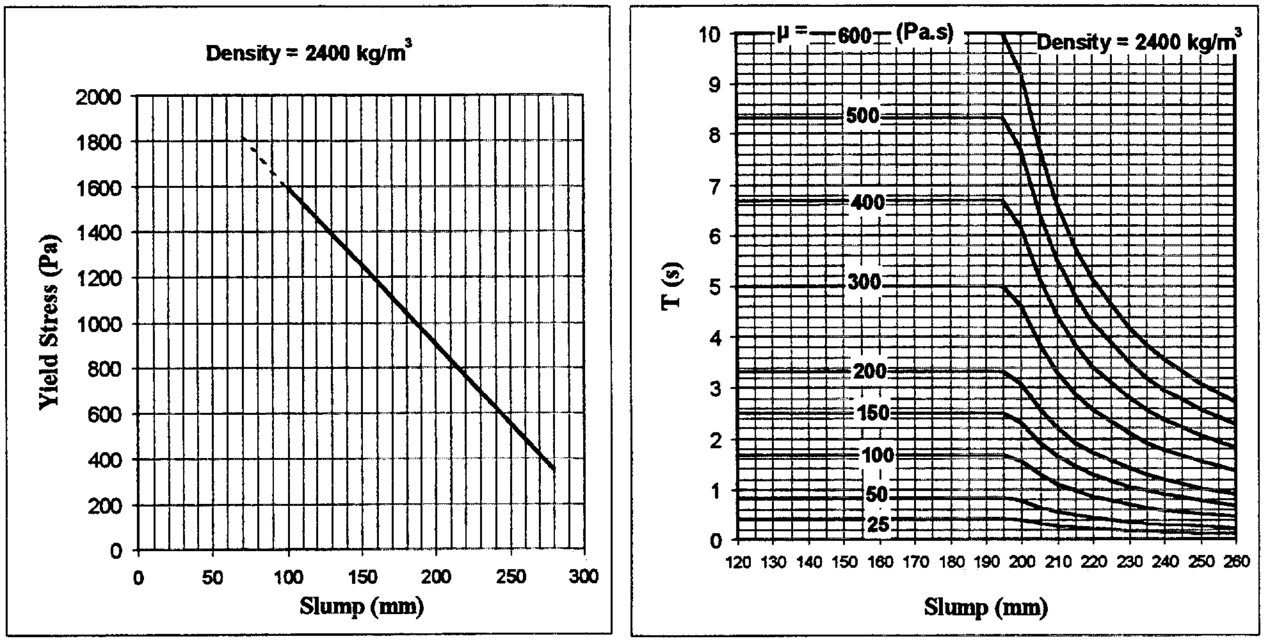

Figure 30. Nomographs for estimating the yield stress and plastic viscosity of concrete from the results of the modified slump test (for a concrete with a density of 2400 kg/m³). From the slump measurements the first graph will give the yield stress. From the second graph by plotting the coordinates of slump and time (T), estimate the plastic viscosity (μ) by interpolating between values corresponding to nearest curves.

6. Summary and Conclusions

The three main goals of this study were to:

- obtain rheological data on concretes of various mixture compositions;
- establish models to link mixture composition with rheological parameters, and
- develop a simple field test for determination of rheological parameters.

To establish a model to link the mixture composition with the rheological properties and to validate such a model, an ambitious experimental plan was developed and conducted. A total of 78 mixtures were made and tested using the slump tests and the rheometer test without vibration. The formulation of the mixtures covers the whole range of mixtures proportions having flow properties measurable by the rheometer. Analysis of the test results led to a modification of the widely-used assumption that concrete behaves as a Bingham fluid. The three-parameter Herschel-Bulkley model was found to be better able to describe the non-linear behavior of fresh concrete than the two-parameter Bingham linear model. The essential argument for using the Herschel-Bulkley model is provided by the self-leveling concretes, for which a calculation of the rheological parameters using the Bingham model often leads to meaningless a negative yield stress. On the contrary, the Herschel-Bulkley model always gives a positive value of yield stress that is reasonably well correlated with the results of the slump test (slump or slump flow depending on the mixture under consideration). Nevertheless, for practical applications, the Bingham model could still be an effective tool, provided that the method of calculating the yield stress and plastic viscosity parameters is changed. Simple modifications of the Bingham equations have been proposed to give better fits to the data.

A model for predicting the rheological properties of the mortars and concretes (yield stress and plastic viscosity) from the mixture composition, and fundamental characteristics of the components was proposed. To test the general validity of the model, it should be applied to other mixtures with different constituent characteristics.

The plastic viscosity was described as a function of the relative volumetric concentration of solids of the mixture in accordance with a model that, for the mixtures tested, proves to be independent of whether a HRWRA or a mineral admixture (silica fume) is present. As for the yield stress, it is expressed in terms of the sum of the relative solid volumetric concentrations of the particles classes, modified by coefficients that take into account the roughness and size of the particles and their capacity to absorb the HRWRA, if present.

The different forms of the two models for yield stress and plastic viscosity explains the absence of a general correlation between yield stress and plastic viscosity, that form the basis for the development of the fresh concrete rheology [1]. It is possible to explain why high-performance concretes have viscosities that are generally higher that those of ordinary concretes. It was found that HRWRA, acting as a water reducer, lowers the yield stress much more than the plastic viscosity. This also allows one to foresee that the optimal granular proportions of concrete for rheological properties will not be the same for ordinary concrete (without HRWRAs) as for self-leveling concretes (with HRWRAs). Finally, in the presence of HRWRA, the contribution of the cement to the yield stress is much reduced. This explains why, for concretes with a very low yield stress and a normal or high plastic viscosity (the case of self-leveling concretes [44]), the optimal composition is rich in fine materials.

The proposed models need to be validated using a larger pool of constituent materials. If and when validated, they can be easily integrated into a computerized system for mixture proportioning. The plastic viscosity can be estimated from measurements of the size distribution and packing density of the materials. The model for estimating yield stress needs to be further validated to determine whether the values of the parameters apply to a whole family of materials or, must be modified when the components are changed.

Finally, a modification of the standard slump test intended to make it possible to evaluate for fresh concretes the two parameters in the Bingham equation is presented. The procedure has been described in detail and the results of tests on 78 mixtures have been reported. The conclusions are as follows:

- From the final slump and the density of the concrete it is possible to estimate the yield stress in the field for a concrete with slumps greater than 100 mm;

- From the slump times and, yield stress and the density of the concrete an estimate can be made of the plastic viscosity for concretes with slumps between 120 mm and 260 mm. The range of application is therefore limited to the slump range of most high-performance concretes, currently being used.

The third objective of study, i.e., to provide a field test to estimate rheological parameters, is thus achieved, at least for one category of concretes. Additional areas of research needed to support the development of a standard test method include the following:

- Evaluation of the repeatability and reproducibility of the modified slump test;

- Verification with a wide range of concrete components of the general applicability of the model linking the slump time to the plastic viscosity should be verified with other concretes made of different components;

- Determination of the value of plastic viscosity and yield stress that are required for placement and finishing under different conditions. It must be noted, however, that while the test provides values of the rheological properties that should be useful for quality control purposes, they are unlikely to be sufficiently precise for achieving an optimum mixture composition.

- The rheometer appears to be a valuable tool for monitoring the changes of concrete rheological behavior with time. It can be used for a wider range of concrete flows than does the modified slump test.

7. Appendixes

Appendix I

Composition of the mixtures without HRWRA (calculated on the basis of an entrapped-air volume of 1%). (*central* mixture in bold.)

Mixtures	Dry Mixture Mass [%]				Composition [$\mathrm{kg/m^3}$]						
	Gravel	Sand	Fine sand	Cement	Gravel	Sand	Fine sand	Cement	Batch water	Free water	w/c
BO1C	45.0	29.0	9.0	17.0	957	617	191	362	210	200	0.553
BO1B'	45.0	29.0	9.0	17.0	952	614	190	360	214	204	0.567
BO1A	45.0	29.0	9.0	17.0	947	611	189	358	218	208	0.581
BO1A'	45.0	29.0	9.0	17.0	943	607	189	356	222	212	0.595
BO1B	**45.0**	**29.0**	**9.0**	**17.0**	**938**	**604**	**188**	**354**	**226**	**216**	**0.610**
BO2A	48.0	30.9	9.6	11.4	1006	648	201	240	215	204	0.850
BO2B	48.0	30.9	9.6	11.4	996	642	199	237	223	212	0.893
BO2C	48.0	30.9	9.6	11.4	986	635	197	235	231	220	0.936
BO3A	24.0	49.3	15.3	11.4	483	993	308	230	244	235	1.020
BO3B	24.0	49.3	15.3	11.4	478	983	305	228	252	243	1.066
BO3C	24.0	49.3	15.3	11.4	473	972	302	226	260	251	1.113
BO4A	57.6	19.3	6.0	17.0	1207	405	126	356	223	212	0.595
BO4C	57.6	19.3	6.0	17.0	1201	403	125	354	227	216	0.610
BO4B	57.6	19.3	6.0	17.0	1194	401	124	352	231	220	0.624
BO5A	22.5	46.2	14.3	17.0	460	944	293	347	240	231	0.666
BO5B	22.5	46.2	14.3	17.0	455	934	290	344	248	239	0.696
BO5C	22.5	46.2	14.3	17.0	450	925	287	340	256	247	0.727
BO6C	0.0	63.4	19.7	17.0	0	1207	375	323	291	284	0.877
BO6B	0.0	63.4	19.7	17.0	0	1193	370	319	299	292	0.914
B06A	0.0	63.4	19.7	17.0	0	1179	366	316	307	300	0.950
BO7C	52.0	17.4	5.4	25.1	1093	367	114	529	230	220	0.416
BO7A	52.0	17.4	5.4	25.1	1081	363	113	523	238	228	0.436
BO7B	52.0	17.4	5.4	25.1	1070	359	111	518	246	236	0.456
BO8C	40.6	26.2	8.1	25.1	851	549	170	527	231	222	0.421
BO8A	40.6	26.2	8.1	25.1	843	543	169	522	239	230	0.440
BO8B	40.6	26.2	8.1	25.1	834	537	167	517	247	238	0.460
BO9A	20.3	41.7	12.9	25.1	413	849	264	512	252	244	0.477
BO9B	20.3	41.7	12.9	25.1	409	840	261	507	260	252	0.498
BO9C	20.3	41.7	12.9	25.1	405	831	258	501	268	260	0.519
BO10C	0.0	57.2	17.7	25.1	0	1107	344	486	289	282	0.580
BO10B	0.0	57.2	17.7	25.1	0	1094	340	481	297	290	0.603
BO10A	0.0	57.2	17.7	25.1	0	1082	336	475	304	298	0.627
BO11A	0.0	51.1	15.9	33.0	0	984	305	635	302	296	0.466
BO11B	0.0	51.1	15.9	33.0	0	973	302	628	310	304	0.484
BO11C	0.0	51.1	15.9	33.0	0	961	298	621	318	312	0.503

Appendix II

Composition of the mixtures with HRWRA (dosage at 1% solid by mass of cement). (Central mixture in bold.)

Mixtures	Dry mixture Mass [%]				Composition [kg/m^3]							
	Gravel	Sand	Fine Sand	Cement	Gravel	Sand	Fine Sand	Cement	Super-plasticizer	Batch water	Free water	w/c
BHP1A	45.0	28.0	8.0	19.0	1015	632	180	429	10.71	159	155	0.362
BHP1A'	45.0	28.0	8.0	19.0	1012	630	180	427	10.68	162	158	0.369
BHP1B	**45.0**	**28.0**	**8.0**	**19.0**	**1009**	**628**	**179**	**426**	**10.65**	**164**	**160**	**0.376**
BHP1B'	45.0	28.0	8.0	19.0	1006	626	179	425	10.62	167	163	0.383
BHP1C	45.0	28.0	8.0	19.0	1003	624	178	423	10.59	169	165	0.390
BHP2A	48.4	30.1	8.6	12.8	1085	675	193	287	7.17	159	152	0.529
BHP2B	48.4	30.1	8.6	12.8	1079	671	192	285	7.13	164	157	0.550
BHP2C	48.4	30.1	8.6	12.8	1072	667	191	283	7.08	169	162	0.571
BHP3A	24.2	49.0	14.0	12.8	523	1058	302	276	6.91	188	182	0.660
BHP3C	24.2	49.0	14.0	12.8	516	1045	299	273	6.82	198	192	0.705
BHP3C'	24.2	49.0	14.0	12.8	507	1026	293	268	6.69	213	207	0.775
BHP4C	57.0	18.7	5.3	19.0	1286	421	120	429	10.72	160	155	0.360
BHP4A	57.0	18.7	5.3	19.0	1278	419	120	426	10.66	165	160	0.374
BHP4B	57.0	18.7	5.3	19.0	1270	416	119	424	10.59	170	165	0.388
BHP5A	21.2	43.0	12.3	23.5	468	947	271	519	12.97	182	181	0.349
BHP5B	21.2	43.0	12.3	23.5	465	941	269	516	12.89	187	186	0.361
BHP5C	21.2	43.0	12.3	23.5	462	935	267	513	12.81	192	191	0.373
BHP6A	0.0	56.0	16.0	28.0	0	1197	342	599	14.97	210	212	0.354
BHP6C	0.0	56.0	16.0	28.0	0	1173	335	587	14.67	226	228	0.389
BHP6B	0.0	56.0	16.0	28.0	0	1164	332	582	14.55	232	234	0.402
BHP7C	50.6	16.6	4.7	28.1	1146	376	107	635	15.89	165	165	0.259
BHP7B	50.6	16.6	4.7	28.1	1139	373	107	632	15.79	170	170	0.269
BHP7A	50.6	16.6	4.7	28.1	1132	371	106	628	15.69	175	175	0.278
BHP8C	40.0	24.9	7.1	28.0	904	563	161	634	15.86	166	166	0.262
BHP8B	40.0	24.9	7.1	28.0	899	559	160	630	15.76	171	171	0.271
BHP8A	40.0	24.9	7.1	28.0	893	556	159	627	15.66	176	176	0.281
BHP9C	20.0	40.4	11.6	28.0	442	895	256	621	15.51	183	184	0.296
BHP9A	20.0	40.4	11.6	28.0	440	890	254	617	15.42	188	189	0.306
BHP9B	20.0	40.4	11.6	28.0	437	884	253	613	15.32	193	194	0.316
BHP10C	0.0	49.2	14.1	36.8	0	1050	300	785	19.63	220	225	0.287
BHP10B	0.0	49.2	14.1	36.8	0	1039	297	777	19.43	228	233	0.300
BHP10A	0.0	49.2	14.1	36.8	0	1028	294	769	19.22	236	241	0.313
BHP11C	0.0	42.6	12.2	45.3	0	901	257	957	23.93	235	244	0.255
BHP11B	0.0	42.6	12.2	45.3	0	891	255	947	23.67	243	252	0.266
BHP11A	0.0	42.6	12.2	45.3	0	881	252	937	23.42	251	260	0.278

Appendix III

Composition of the mixtures with intermediate amounts of HRWRAs and concretes with silica fume. SF = silica fume (the mass indicated is for the slurry) and SP = HRWRA

Mixtures	Dry Mixture Mass [%]					Composition [kg/m^3]								
	Gravel	Sand	Fine Sand	Cement	SF	Gravel	Sand	Fine Sand	Cement	SF	SP	Batch water	Free Water	w/c
80%BO	45.0	28.8	8.8	17.4		952	609	186	369		2.13	214	205	0.556
60%BO	45.0	28.6	8.6	17.8		966	614	184	383		4.26	201	194	0.506
40%BO	45.0	28.4	8.4	18.2		980	618	183	397		6.39	189	182	0.459
20%BO	45.0	28.2	8.2	18.6		995	623	181	412		8.52	177	171	0.416
FS 7,5	44.2	27.5	7.9	19.1	1.43	1000	622	178	431	60	14	125	150	0.348
FS 15	43.3	27.0	7.7	19.1	2.87	988	615	176	435	121	17	87	142	0.326
FS 22,5	42.5	26.5	7.6	19.2	4.31	973	605	173	438	183	21	50	136	0.310
FS 30	41.7	25.9	7.4	19.2	5.76	951	592	169	438	244	24	20	136	0.310

Appendix IV

Result of the tests for mixtures without HRWRA. Only the mixtures designated in bold are in the range of applicability of the rheometer.

Mixtures		Slump cone		Bingham		Herschel-Bulkley				Observ.*		Comments
	Specific gravity	Slump (mm)	Time (s)	Yield (Pa)	Visc. (Pa·s)	Yield (Pa)	a ($Pa{\cdot}s^b$)	b	μ' (Pa·s)	Bleed	Segr.	
BO1C	2.33	80		1717	174	1804	111	1.23	156			
BO1B'	2.33	100		1489	163	1599	86	1.33	140			
BO1A	2.31	130	2.15	1219	160	1341	74	1.40	134			
B01A'	2.32	165	1.51	881	133	983	62	1.40	111	1		
BO1B	2.30	225	0.85	802	84	778	102	0.90	89	1		
BO2A	2.28	55		1387	285	1612	132	1.39	236			
BO2B	2.27	125	1.55	1037	163	1162	74	1.41	137	2		
BO2C	2.26	170	1.73	1185	130	1306	46	1.55	105	3		cone sheared
BO3A	2.24	35		1385	258	1690	60	1.77	191	1		
BO3B	2.21	60		1206	200	1460	36	1.92	145	2		
BO3C	2.19	185	1.16	799	127	949	27	1.84	96	3		
BO4A	2.29	80		1906	147	2019	70	1.38	122		1	sheared cone + lack of cohesion
BO4C	2.31	135	2.42	1676	209	1972	28	2.09	144		1	lack of cohesion
BO4B	2.29	185	2	1913	223	2151	57	1.75	176		1	lack of cohesion
BO5A	2.26	95		1008	208	1234	55	1.72	161			
BO5B	2.26	95	1.9	951	172	1071	87	1.35	146			
BO5C	2.22	160	1.43	839	90	906	43	1.39	76	1		
BO6C	2.11	55		2216	73	2344	1	3.39	50			
BO6B	2.12	70		2036	77	2163	3	2.84	50			
B06A	2.10	65		2132	96	2273	11	2.20	67			
BO7C	2.33	12	2.24	1473	183	1665	53	1.66	143		1	
BO7A	2.31	155	1.91	1147	147	1281	54	1.53	119			
BO7B	2.30	195	1.4	752	117	869	38	1.61	93			
BO8C	2.33	105	1.99	1688	146	1841	42	1.66	114			
BO8A	2.33	170	1.57	1090	111	1115	93	1.09	106			
BO8B	2.31	205	1.06	888	59	901	50	1.09	56			
BO9A	2.27	105	2.57	1432	75	1496	30	1.48	62			
BO9B	2.27	150	1.15	1068	73	1137	26	1.55	59			
BO9C	2.26	225	0.67	733	34	771	9	1.74	27			
BO10C	2.17	80		1702	52	1754	17	1.61	42			
BO10B	2.12	170	0.96	1123	35	1049	96	0.57	52			
BO10A	2.15	210	0.92	1024	46	1061	20	1.45	38			
BO11A	2.17	115	1.22	1195	48	1263	5	2.22	34			
BO11B	2.19	175	0.92	976	36	1001	18	1.36	31			
BO11C	2.20	230	0.91	731	25	764	4	1.97	19			

Note: * The numbers (0 to 3) are qualitative ranking (0= good and 3 = worst case).

Appendix V

Result of the tests for mixtures with HRWRA. Only the mixtures designated in bold are in the range of applicability of the rheometer

Mixtures		Slump cone			Bingham		Herschel-Bulkley				Obser. *		Comments
	Specific Gravity	Slump (mm)	Time (s)	Spread (mm)	Yield (Pa)	Visc. (Pa·s)	Yield (Pa)	a (Pa·s^b)	b	μ' (Pa·s)	Bleed.	Segr.	
BHP1A	2.38	*215*	15.97		649	499	759	417	1.09	476	1		
BHP1A'	2.38	180	10.19		593	517	774	385	1.15	479	1		sheared cone
BHP1B	2.38	205	7.03		473	530	608	430	1.10	501	2		
BHP1B'	2.38		5.34		122	427	537	147	1.56	338	2		
BHP1C	2.37	235			141	439	471	205	1.40	370	3		
BHP2A	2.27	5										2	
BHP2B	2.30	5										2	
BHP2C	2.33	10									1	2	
BHP3A	2.20	0											wet dirt
BHP3C	2.19	0											id.
BHP3C'	2.20	10									3		
BHP4C	2.41	135	11.93								1	3	
BHP4A	2.37	150	7.22		1216	544	1741	190	1.54	425	1	2	lack of cohesion
BHP4B	2.40	120	12.32		893	437	1457	87	1.83	301	3	2	
BHP5A	2.25	150	12.97		1055	519	863	665	0.88	561			
BHP5B	2.32	225	4.95		363	589	476	506	1.07	565	1		
BHP5C	2.32	260	2.04	590	115	401	413	191	1.39	338	2		
BHP6A	*2.00*	45									1		
BHP6C	2.22	145	2.17		200	303	500	99	1.59	240	2		
BHP6B	2.21	200			465	424	877	145	1.56	336	3		
BHP7C	2.43	240	2.97	550								3	Pile of gravel[6]
BHP7B	2.44	245	2.08	640	90	586	467	316	1.32	508	1	3	id.
BHP7A	2.40	250	1.82	670	61	535	585	181	1.57	422	2	2	id.
BHP8C	2.40	265	4.27	560	-452	1960	675	792	1.88	2956			reduced shear rate
BHP8B	2.39	285	1.83	700	-373	879	457	269	1.73	795	1	1	
BHP8A	2.37	290		750	-147	488	385	132	1.70	376	2	1	
BHP9C	2.37	275	2.56	630	-73	802	548	336	1.52	726	0.5		
BHP9A	2.29	*270*	1.8	620	47	528	268	367	1.18	480	1		
BHP9B	2.35	285	1.24	760	-85	322	256	92	1.67	252	2		
BHP10C	2.34	280	1.56	740	145	694	314	560	1.12	669			reduced shear rate
BHP10B	2.31	285	1.37	790	204	371	327	281	1.14	345	2		
BHP10A	*2.13*	290	1.06	760	250	155	323	101	1.21	139	1		
BHP11C	2.37	290	1.22	850	86	695	193	615	1.06	672			
BHP11B	2.34	290	1.37	890	-123	429	279	153	1.55	346			
BHP11A	2.35	295	1.32	950	-14	297	96	217	1.16	274	2		

Note: * The numbers (0 to 3) are qualitative ranking (0= good and 3 = worst case).

---

[6] At the center of the spread of concrete after the slump test.

Appendix VI

Result of the tests for concretes with intermediate dosages of HRWRA and silica-fume.

Mixtures		Slump Cone			Bingham		Herschel-Bulkley				Observ.*		
	Specific gravity	Slump. (mm)	Time (s)	Spread (mm)	Yield (Pa)	Visc. (Pa·s)	Yield (Pa)	a ($Pa{\cdot}s^b$)	b	μ' (Pa·s)	Bleed	Segr.	Comments
80%BO	*2.25*	240	0.63		432	121	451	106	1.07	116	2		
60%BO	2.33	235	1.02	660	294	205	353	161	1.12	192	3		Pile of aggregates
40%BO	2.36	220	1.97	600	77	295	312	132	1.42	245	3		Pile of aggregates
20%BO	2.39	220	2.93		33	394	448	115	1.66	308	3		
FS 7,5	2.40	245	2.46		303	449	594	243	1.32	387			
FS 15	2.43	235	2.66		312	423	527	267	1.23	378			
FS 22,5	2.42	230	3.31		625	418	748	327	1.13	393			
FS 30	2.45	215			1117	397	1068	435	0.96	408			

Note: * The numbers (0 to 3) are qualitative ranking (0= good and 3 = worst case).

Appendix VII

Calculations of the theoretical values of the rheological properties for various mixtures

Mixtures	Φ	$\Phi*$	$\Phi/\Phi*$	K'_g	K'_s	K'_c	K'_{sf}	τ_0 (Pa) exp.	τ_0 (Pa) mod.	μ (Pa·s) exp.	μ (Pa·s) mod.
BO1C	0.7980	0.8532	0.9353	1.617	2.267	1.695	0				
BO1B'	0.7939	0.8532	0.9305	1.591	2.213	1.637	0	1599	1524	140	144
BO1A	0.7899	0.8532	0.9258	1.566	2.162	1.583	0	1341	1341	134	127
B01A'	0.7859	0.8532	0.9211	1.542	2.112	1.531	0	983	1188	111	112
BO1B	0.7818	0.8532	0.9163	1.518	2.064	1.483	0	778	1058	89	98
BO2A	0.7940	0.8542	0.9296	1.886	2.64	0.994	0				
BO2B	0.7860	0.8542	0.9201	1.82	2.506	0.936	0	1162	970	137	109
BO2C	0.7779	0.8542	0.9107	1.759	2.383	0.883	0				
BO3A	0.7627	0.8314	0.9174	0.645	3.522	0.843	0				
BO3B	0.7546	0.8314	0.9077	0.63	3.344	0.798	0				
BO3C	0.7466	0.8314	0.8980	0.616	3.181	0.757	0	949	730	96	60
BO4A	0.7859	0.8479	0.9268	2.497	1.484	1.484	0				
BO4C	0.7818	0.8479	0.9221	2.447	1.451	1.438	0	1972	971	144	115
BO4B	0.7778	0.8479	0.9173	2.398	1.419	1.395	0				
BO5A	0.7665	0.8353	0.9176	0.583	3.061	1.392	0	1234	1345	161	102
BO5B	0.7584	0.8353	0.9079	0.57	2.919	1.31	0	1071	1066	146	79
BO5C	0.7503	0.8353	0.8982	0.558	2.788	1.236	0	906	860	76	61
BO6C	0.7136	0.8054	0.8861	0	3.596	1.02	0		983		
BO6B	0.7051	0.8054	0.8754	0	3.423	0.966	0				
B06A	0.6970	0.8054	0.8654	0	3.273	0.919	0				
BO7C	0.7778	0.8340	0.9326	1.799	1.117	2.436	0	1665	1635	143	152
BO7A	0.7696	0.8340	0.9228	1.741	1.075	2.27	0	1281	1246	119	117
BO7B	0.7615	0.8340	0.9131	1.686	1.036	2.124	0	869	977	93	90
BO8C	0.7758	0.8333	0.9309	1.18	1.584	2.462	0	1841	1823	114	145
BO8A	0.7681	0.8333	0.9217	1.15	1.527	2.302	0	1115	1381	106	114
BO8B	0.7600	0.8333	0.9120	1.12	1.47	2.152	0	901	1074	56	88
BO9A	0.7534	0.8225	0.9160	0.476	2.27	2.137	0	1496	1495	62	98
BO9B	0.7454	0.8225	0.9062	0.467	2.181	2.003	0	1137	1167	59	75
BO9C	0.7373	0.8225	0.8964	0.457	2.098	1.883	0	771	933	27	58
BO10C	0.7152	0.7994	0.8946	0	2.909	1.68	0				
BO10B	0.7071	0.7994	0.8845	0	2.792	1.588	0				
BO10A	0.6990	0.7994	0.8744	0	2.683	1.504	0	1061	761	38	32
BO11A	0.7010	0.7854	0.8926	0	2.207	2.23	0	1263	1172	34	52
BO11B	0.6929	0.7854	0.8823	0	2.13	2.103	0	1001	939	31	40
BO11C	0.6848	0.7854	0.8720	0	2.058	1.987	0	764	768	19	30
BHP1A	0.8434	0.8620	0.9785	1.913	2.678	2.582	0	759	759	476	518
BHP1A'	0.8409	0.8620	0.9755	1.893	2.63	2.51	0	774	717	479	479
BHP1B	0.8384	0.8620	0.9726	1.873	2.591	2.439	0	608	660	501	443
BHP1B'	0.8359	0.8620	0.9697	1.854	2.549	2.373	0	537	625	338	410

BHP1C	0.8333	0.8620	0.9667	1.835	2.508	2.31	0	471	578	370	379
BHP2A	0.8467	0.8610	0.9834	2.433	3.53	1.565	0				
BHP2B	0.8416	0.8610	0.9775	2.373	3.391	1.488	0				
BHP2C	0.8366	0.8610	0.9716	2.315	3.261	1.417	0				
BHP3A	0.8158	0.8399	0.9713	0.761	4.827	1.271	0				
BHP3C	0.8057	0.8399	0.9592	0.738	4.452	1.165	0				
BHP3C'	0.7905	0.8399	0.9412	0.706	3.979	1.031	0				
BHP4C	0.8439	0.8564	0.9855	3.238	1.878	2.486	0				
BHP4A	0.8389	0.8564	0.9796	3.146	1.819	2.353	0	1741	669	425	534
BHP4B	0.8338	0.8564	0.9737	3.058	1.763	2.232	0	1457	585	301	456
BHP5A	0.8171	0.8422	0.9702	0.6	3.254	2.869	0	863	663	561	415
BHP5B	0.8120	0.8422	0.9642	0.592	3.154	2.719	0	476	579	565	354
BHP5C	0.8070	0.8422	0.9582	0.584	3.06	2.582	0	413	510	338	301
BHP6A	0.7859	0.8127	0.9670	0	3.814	2.914	0				
BHP6C	0.7697	0.8127	0.9471	0	3.473	2.504	0	500	506	240	224
BHP6B	0.7636	0.8127	0.9396	0	3.359	2.375	0	877	442	336	183
BHP7C	0.8337	0.8438	0.9881	2.085	1.274	4.194	0				
BHP7B	0.8287	0.8438	0.9821	2.042	1.242	3.932	0	467	309	508	571
BHP7A	0.8236	0.8438	0.9761	2	1.212	3.699	0	585	276	422	487
BHP8C	0.8322	0.8433	0.9869	1.359	1.818	4.278	0				
BHP8B	0.8272	0.8433	0.9809	1.337	1.771	4.005	0	457	339	795	553
BHP8A	0.8221	0.8433	0.9749	1.314	1.726	3.764	0	385	303	376	471
BHP9C	0.8142	0.8338	0.9765	0.537	2.745	3.673	0	548	485	726	492
BHP9A	0.8092	0.8338	0.9705	0.531	2.67	3.464	0	268	427	480	419
BHP9B	0.8041	0.8338	0.9644	0.524	2.598	3.277	0	256	380	252	356
BHP10C	0.7727	0.7989	0.9672	0	2.656	3.954	0	314	344	669	384
BHP10B	0.7646	0.7989	0.9571	0	2.557	3.639	0	327	291	345	293
BHP10A	0.7566	0.7989	0.9470	0	2.465	3.365	0	323	250	139	223
BHP11C	0.7535	0.7786	0.9678	0	1.87	4.735	0	193	204	672	390
BHP11B	0.7455	0.7786	0.9574	0	1.812	4.349	0	279	173	346	295
BHP11A	0.7374	0.7786	0.9471	0	1.757	4.017	0	96	152	274	224
80%BO	0.7931	0.8557	0.9269					451		116	130
60%BO	0.8044	0.8590	0.9365					353		192	169
40%BO	0.8158	0.8609	0.9476					312		245	227
20%BO	0.8271	0.8621	0.9594					448		308	311
FS 7.5	0.8485	0.8702	0.9750	1.616	2.656	2.442	0.154	594	746	387	473
FS 15	0.8566	0.8806	0.9727	1.556	2.512	2.376	0.349	527	879	378	444
FS 22.5	0.8626	0.8875	0.9720	1.487	2.349	2.265	0.59	748	1037	393	436
FS 30	0.8626	0.8924	0.9666	1.393	2.13	2.05	0.844	1068	1129	408	378

8. ACKNOWLEDGEMENTS

The authors wish to specially thank John Winpigler of the National Institutes of Standards and Technology for his participation in the preparation of materials and for the conduct of the rheological tests and Frank Davis, also from NIST, for repair of the concrete mixer. They also have not forgotten the help shown by Pierre Roussel (LCPC) for the tests to identify the binders and by the department of the Physics and Chemistry of Materials of LCPC for the analyses of the components. Finally, they wish to mention the contributions of W.R. Grace Co. which provided the mixer and the HRWRA and the Elkem Company which provided the silica fume. We also would like to thank Drs. James Clifton, Edward Garboczi and Nicholas Carino for the review of this paper.

9. REFERENCES

1 TATTERSALL, G.H. (1991), "Workability and Quality-Control of Concrete," E & FN SPON, London.
2 WALLEVIK, O. (1990), "Den ferske betongens reologi og anvendelse pa betong med og uten tilsetning av silikastov", PhD Thesis, University of Trondheim NTH.
3 HU, C., DE LARRARD, F., GJϕRV, O.E. (1995), "Rheological Testing and Modelling of Fresh High-Performance Concrete", Materials and Structures, Vol. 28, pp. 1-7.
4 DE LARRARD, F., HU, C., SEDRAN, T., SITZKAR, J.C., JOLY, M., CLAUX, F., DERKX, F. (1997), "A New Rheometer for Soft-to-Fluid Fresh Concrete", ACI Materials Journal, Vol. 94, No. 3, May-June, pp. 234-243.
5 DE LARRARD, F., SEDRAN, T., HU, C., SITZKAR, J.C., JOLY, M., DERKX, F. (1996), "Evolution of the workability of superplasticized concretes: assessment with BTRHEOM rheometer", Proceedings of the International RILEM Conference on Production Methods and Workability of Concrete, Paisley, edited by P.J.M. Bartos, D.L. Marrs and D.J. Cleland, pp. 377-388, June.
6 HUYNH, T. (1996), "La compatibilité ciment-adjuvant. Etude bibliographique", Bulletin des Laboratoires des Ponts et Chaussées, N° 206, pp. 63-74, November-December.
7 HU, C. (1995), "Rhéologie des bétons fluides", Etudes et Recherches des Laboratoires des Ponts et Chaussées, OA 16, 203 p., Paris, France
8 DE LARRARD, F., SZITKAR, J.C., HU, C., JOLY, M. (1994), "Design of a rheometer for fluid concretes", Proceedings of the International RILEM workshop Special Concretes: Workability and Mixing, P.J.M. Bartos ed., E & FN SPON, pp. 201-208.
9 TANIGAWA, Y., MORI, H. (1989),"Analytical Study on Deformation of Fresh Concrete", Journal of Engineering Mechanics, Vol. 115, No.3, March
10 TANIGAWA, Y., MORI, H., WATANABE, K. (1991),"Analytical and Experimental Studies on Casting of Fresh Concrete Into Wall Form", Transcription of the Japan Concrete Society, Vol.13
11 "Standard Test Method for Specific Gravity and Absorption of Fine Aggregate" ASTM C128 -93, Annual Book of ASTM Standards Vol. 04.02

12 "Standard Test Method for Specific Gravity and Absorption of Coarse Aggregate" ASTM C127 -88, Annual Book of ASTM Standards Vol. 04.02

13 SEDRAN, T., DE LARRARD, F. (1996), "RENé-LCPC: a software to optimize the mix-design of High-Performance Concrete", BHP 96, 4th International Symposium on the Utilization of High-Strength/High-Performance Concrete, edited by F. de Larrard and R. Lacroix, Paris, May, pp. 169-178.

14 "Standard Specification for Portland Cement" ASTM C150 -95, Annual Book of ASTM Standards Vol. 04.01

15 EN 196-1 (1987) "Methods of testing cement: Determination of strength"

16 "Standard Test Method for Unit Weight, Yield and Air Content (Gravimetric) of Concrete" ASTM C138 -92, Annual Book of ASTM Standards Vol. 04.02

17 "Standard Test Method for Slump of Hydraulic Cement concrete" ASTM C143 -90, Annual Book of ASTM Standards Vol. 04.02

18 TANG, F. J., BHATTACHARJA, S. (1996), "Development of an Early Stiffening Test", PCA Research and Development, RP 346.

19 DE LARRARD, F., BOSC, F., CATHERINE, C., DEFLORENNE, F. (1997), "The AFREM Method for the Mix-design of High-Performance Concrete", Materials and Structures, Vol. 30, No. 201, pp. 439-446, August-September.

20 YONEZAWA, T., IZUMI, I., OKUNO, T., SUGIMOTO, M., SHIMONO, T., ASAKURA, E. (1992), "Reducing the Viscosity of High-Strength Concrete Using Silica Fume", 4th CANMET/ACI Conference on Fly Ash, Silica Fume, Slag and Natural Pozzolans in Concrete, Supplementary papers, Istanbul, May.

21 COUSSOT, P., PIAU, J.-M. (1995), "A large-scale field coaxial cylinder rheometer for the study of the rheology of natural coarse suspensions", Journal of Rheology, 39, pp.104-123

22 BIRD, R.B., DAI, G.C., YARUSSO, B.J. (1982), "The rheology and flow of viscoplastic materials", Rev. Chem.Eng., 1, 1-70.

23 PASHIAS, N., BOGER, D.V., SUMMERS, J., GLENISTER, D.J. (1996), "A fifty cent rheometer for yield stress measurement", J. Rheol. 40 (6), November/December

24 SEDRAN, T. (1995), "Les bétons autonivelants. Synthèse bibliographique", Bulletin de Liaison des Laboratoires des Ponts et Chaussées, N°196, pp. 53-60, Mars-Avril

25 FARRIS, R.J. (1968), "Prediction of the Viscosity of Multimodal Suspensions from Unimodal Viscosity Data", Transactions of the Society of Rheology, Vol.12, No.2, pp. 281-301.

26 CHANG, C., POWELL, R.L. (1994),"Effect of particle size distributions on the rheology of concentrated bimodal suspensions", Journal of Rheology, Vol. 38, No.1, pp. 85-98, January/February.

27 STOVALL, T., DE LARRARD, F., BUIL ,M. (1986), "Linear Packing Density Model of Particule Mixtures. Powder Technology", Vol.48, N°1, September.

28 DE LARRARD, F., SEDRAN, T., ANGOT, D. (1994^{a}), "Prévision de la compacité des mélanges granulaires par le modèle de suspension solide. I: Fondements théoriques et calibration du modèle", Bulletin de Liaison des Laboratoires des Ponts et Chaussées, N°194, Novembre-Décembre, 1994.

29 DE LARRARD, F., SEDRAN, T., ANGOT, D. (1994^{b}), "Prévision de la compacité des mélanges granulaires par le modèle de suspension solide. II: Validations et cas des mélanges confinés", Bulletin de Liaison des Laboratoires des Ponts et Chaussées, N°194, Novembre-Décembre, 1994

30 JOISEL A. (1952), "Composition des bétons hydrauliques", Annales de l'ITBTP, 5ème année, No. 58, Série : Béton. Béton armé (XXI), October.

31 KANTHA RAO V.V.L., KRISHNAMOOTHY S. (1993), "Aggregate Mixtures for Least-Void Content for Use in Polymer Concrete", Cement, Concrete and Aggregates, CCAGDP, Vol.15, No.2, Winter, pp. 97-107.

32 LECOMTE, A., ZENNIR, A., "Modèle de suspension solide et granulats calcaires de Lorraine", to appear in Bulletin des Laboratoires des Ponts et Chaussées.

33 DE LARRARD, F. (1998), "Concrete Mixtures Proportioning: a Scientific Approach", Modern Concrete Technology Series, E&FN SPON, to be published.

34 PERLO, S. (1995), "Validation du modèle de suspension solide pour les coulis à base de ciment et d'addition minérale", Mémoire de DEA, ENS de Cachan, Juin.

35 SEDRAN, T., private communication, LCPC, 1997

36 HOBBS, D.W. (1976), "Influence of Aggregate Volume Concentation Upon the Workability of Concrete and Some Predictions from the Viscosity-Elasticity Analogy", Magazine of Concrete Research, Vol.28, No.97, December.

37 MURATA, J., KIKUKAWA, H. (1992),"Viscosity Equation for Fresh Concrete", ACI Materials Journal, Vol.89, No.3, May-June.

38 SZECSY, R.S. (1997), "Concrete Rheology", PhD Thesis, University of Illinois at Urbana-Champaign.

39 FERRARIS, C.F., GAIDIS, J.M. (1992), "Connection between the Rheology of Concrete and Rheology of Cement Paste", ACI Materials Journal, Vol.89, No.4, pp.388-393

40 DAY, K.W. (1995), "Concrete Mix-Design, Quality Control and Specification", E & FN SPON, 350 p..

41 BUIL, M., WITIER, P., DE LARRARD, F., DETREZ, M., PAILLERE, A.-M. (1986), "Physico-Chemical Mechanism of the Action of the Naphtalene-Sulfonate Based HRWRAs on Silica Fume Concretes", 2nd International ACI-CANMET Conference on Fly Ash, Silica Fume, Slag and Natural Pozzolans in Concrete, ACI SP 91, Madrid

42 FERRARIS, C.F. (1996), "Measurement of Rheological Properties of High-Performance Concrete: State-of-the-Art Report", National Institute of Standards and Technology, NISTIR 5869, 33 p., July.

43 BARTOS, P. (1992), "Fresh Concrete: Properties and Tests", Elsevier

44 SEDRAN, T., DE LARRARD, F. (1996), "Mix-Design of Self-Compacting Concrete", Proceedings of the International RILEM Conference on Production Methods and Workability of Concrete, Paisley, edited by P.J.M. Bartos, D.L. Marrs and D.J. Cleland, pp. 439-450, June.